Coastwide Trends in Seagrass Cover and Condition in Texas Waters

Victoria M. Congdon and Kenneth H. Dunton
The University of Texas at Austin Marine Science Institute
750 Channel View Drive, Port Aransas, TX 78373

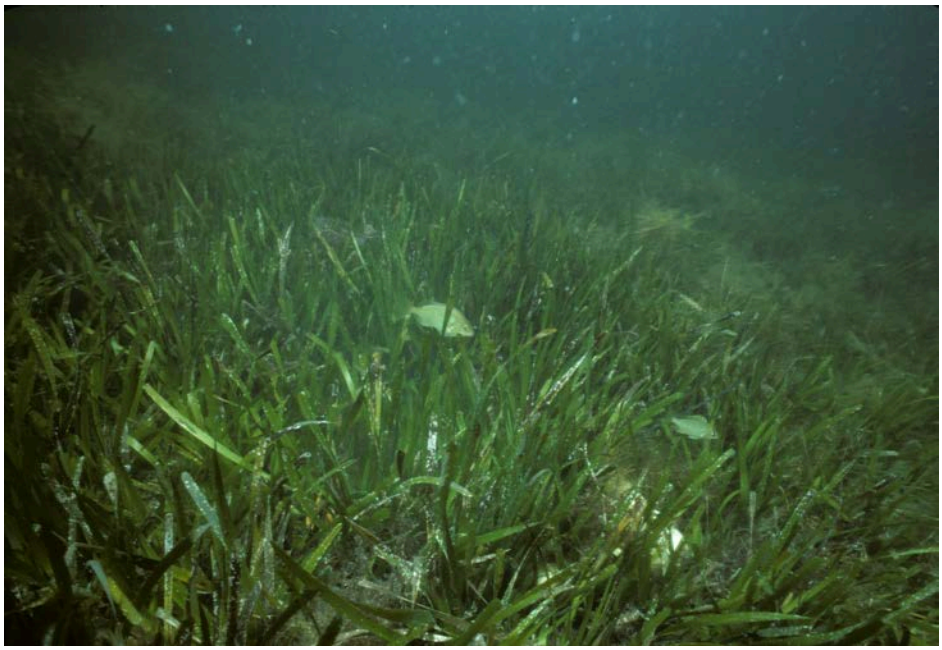

A report funded by a Texas Coastal Management Program grant approved by the Texas Land Commissioner pursuant to National Oceanic and Atmospheric Administration award No. NA17NOS4190139.

Principal Investigator

Kenneth H. Dunton
University of Texas at Austin Marine Science Institute
750 Channel View Drive, Port Aransas, TX 78373
Phone: (361) 749-6744
Fax: (361) 749-6777
E-mail: ken.dunton@utexas.edu

Draft Final Report Submitted by
Victoria M. Congdon
Kenneth H. Dunton

13 October 2019
GLO Cycle 22 Contract: 18-083-000-A592

Project Partners

TABLE OF CONTENTS

PROJECT SUMMARY

This report details the results of the Texas Seagrass Monitoring Program following the survey of 567 and 679 sampling stations during the summer and fall of 2017 and 2018, respectively. Sampling station locations were selected in seagrass meadows that were mapped using remotely sensed data obtained from the 2004/2007 NOAA Benthic Habitat Assessment. Stations were spatially distributed among five estuarine systems: Trinity-San Jacinto, Guadalupe, Mission-Aransas, Nueces, and Laguna Madre. These five estuarine systems contain 100% of the seagrasses along the Texas coast. The 2017 and 2018 field sampling effort implemented Tier-2 protocols, which are intended to provide rapid assessments of hydrography, seagrass coverage, species distributions and plant physiological conditions. We illustrated the data obtained from the field survey using geographic information systems (GIS) in order to evaluate spatial relationships in measured hydrographic and seagrass parameters. The Tier-2 sampling program identified regions exhibiting changes in seagrass species composition and distribution, and thoroughly evaluated the seagrass habitat described in the 2004/2007 NOAA Benthic Habitat Assessment. In addition, collaboration efforts with the Texas Parks and Wildlife, and the Texas Commission on Environmental Quality allowed for the sampling of seagrasses spanning the entire Texas coast.

INTRODUCTION

In 1999, the Texas Parks and Wildlife Department (TPWD), along with the Texas General Land Office (TGLO) and the Texas Commission on Environmental Quality (TCEQ), drafted a Seagrass Conservation Plan that proposed, among other things, a seagrass habitat monitoring program (Pulich and Calnan 1999). One of the main recommendations of this plan was to develop a coast wide monitoring program. In response, the Texas Seagrass Monitoring Plan (TSGMP) proposed a monitoring effort to detect changes in seagrass ecosystem conditions prior to actual seagrass mortality (Pulich et al. 2003). However, implementation of the plan required additional research to specifically identify the environmental parameters that elicit a seagrass stress response and the physiological or morphological variables that best reflect the impact of these environmental stressors.

Numerous researchers have related seagrass health to environmental stressors; however, these studies have not arrived at a consensus regarding the most effective habitat quality and seagrass condition indicators. Kirkman (1996) recommended biomass, productivity, and density for monitoring seagrass whereas other researchers focused on changes in seagrass distribution as a function of environmental stressors (Dennison et al. 1993; Livingston et al. 199; Koch 2001; Fourqurean et al. 2003). The consensus among these studies revealed that salinity, depth, light, nutrient concentrations, sediment characteristics, and temperature were among the most important variables that produced a response in a measured seagrass indicator. The relative influence of these environmental variables is likely a function of the seagrass species in question, the geographic location of the study, hydrography, methodology, and other factors specific to local climatology. Because no generalized approach can be extracted from previous research, careful analysis of regional seagrass ecosystems is necessary to develop an effective monitoring program for Texas.

Conservation efforts should seek to develop a conceptual model that outlines the linkages among seagrass ecosystem components and the role of indicators as predictive tools to assess the seagrass physiological response to stressors at various temporal and spatial scales. Tasks for this objective include the identification of stressors that arise from human-induced disturbances, which can result in seagrass loss or compromise plant physiological condition. For example, stressors that lead to higher water turbidity and light attenuation (e.g. dredging and shoreline erosion) are known to result in lower below-ground

seagrass biomass and alterations to sediment nutrient concentrations. It is therefore necessary to evaluate long-term light measurements, the biomass of above- versus below-ground tissues and the concentrations of nutrients, sulfides and dissolved oxygen in sediment porewater when examining the linkages between light attenuation and seagrass health.

This study implements a program for monitoring seagrass meadows in Texas coastal waters following protocols that evaluate seagrass condition based on landscape-scale dynamics. These protocols adhere to the hierarchical strategy for seagrass monitoring outlined by Neckles et al. (2011) and serve to establish quantitative relationships between physical and biotic parameters that ultimately control seagrass condition, distribution, persistence, and overall health. Our monitoring approach follows a broad template adopted by several federal and state agencies across the country, but which is uniquely designed for Texas (Dunton et al. 2011) and integrates plant condition indicators with landscape feature indicators to detect and interpret seagrass bed disturbances.

The objectives of this study were to (1) implement long-term monitoring to detect environmental changes with a focus on the ecological integrity of seagrass habitats, (2) provide insight to the ecological consequences of these changes, and (3) help decision makers (e.g. various state and federal agencies) determine if the observed change necessitates a revision of regulatory policy or management practices. We defined ecological integrity as the capacity of the seagrass system to support and maintain a balanced, integrated, and adaptive community of flora and fauna including its characteristic foundation seagrass species. Ecological integrity was assessed using a suite of condition indicators (physical, biological, hydrological, and chemical) measured annually on wide spatial scales.

The primary questions addressed in the 2017-2018 annual Tier-2 surveys include:

1) What are the spatial and temporal patterns in the distribution of seagrasses over annual scales?
2) What are the characteristics of these plant communities, including their species composition and percent cover?
3) How are any changes in seagrass percent cover and species composition, related to measured characteristics of water quality?

METHODS

Sampling Summary

Tier-2 protocols, which are considered Rapid Assessment sampling methods, are adapted from Neckles et al. (2011). Tier-2 sampling was conducted July to late-November in 2017 and July to early-December in 2018. For statistical rigor, a repeated measures design with fixed sampling stations was implemented to maximize our ability to detect future change. Neckles et al. (2011) demonstrated that the Tier-2 approach, when all sampling stations are considered together within a regional system, results in > 99% probability that the bias in overall estimates will not interfere with detection of change.

Site Selection

The Tier-2 sampling program is intended to compliment ongoing remote sensing efforts. Sites were therefore selected from vegetation maps generated with aerial and satellite imagery during the 2004/2007 NOAA Benthic Habitat Assessment. The vegetation maps were then tessellated using polygons, and sample locations were randomly selected within each polygon (Figures 1 and 2). Only polygons containing > 50% seagrass coverage were included in 2017 and 2018 sampling efforts in the Mission-Aransas National Estuarine Research Reserve, Corpus Christi Bay, Upper Laguna Madre, Lower Laguna Madre and San Antonio Bay. Polygons containing > 10% seagrass coverage in Christmas and West Bays were used in 2018 sampling efforts. The Mission-Aransas National Estuarine Research Reserve and Corpus Christi Bay regions were reported together as one region, Coastal Bend (CB), whereas Upper and Lower Laguna Madre were referred to as ULM and LLM, respectively. Additionally, San Antonio Bay (SAB) was reported as one region, and Christmas and West Bays were combined into Galveston Bay (GB). In 2017, we sampled the Coastal Bend, Upper Laguna Madre and Lower Laguna Madre. In 2018, we sampled San Antonio Bay and Galveston Bay, in addition to the Coastal Bend, Upper Laguna Madre and Lower Laguna Madre.

Water Quality

In the field, all sampling stations were located within a 10 m radius of the pre-determined station coordinates using a handheld GPS device. Upon arrival to each station, hydrographic measurements including temperature, salinity, dissolved oxygen, chlorophyll fluorescence and pH were collected with a YSI 6920 data sonde. We measured the depth of the water column using a precision depth recorder and estimated water transparency with a secchi disk. Water samples were obtained at each station for determination of Total Suspended Solid (TSS) concentration (See Appendix A.1). Water transparency was derived from measurements of photosynthetically active radiation (PAR) using two LI-COR spherical quantum scalar sensors attached to a lowering frame (See Appendix A.2). All sonde measurements and water samples were obtained prior to the deployment of benthic sampling equipment. In addition, Onset HOBO Conductivity Loggers (model U-24-002-C) were deployed: November 2016 – December 2018 near Padre Island National Seashore (Bird Island) in Upper Laguna Madre (27°24'N, -97°20'W; Figure 3); September 2016 – August 2018 in Nine Mile Hole in Upper Laguna Madre (27°1'N, -97°25'W; Figure 4); and March 2016 – July 2018 near South Padre Island in Lower Laguna Madre (26°6'N, -97°11'W; Figure 5). Conductivity and temperature data were collected hourly and converted to salinity values using HOBOware Pro software.

Seagrass Coverage

Species composition and coverage were obtained from four replicate quadrat samples per station at each of the four cardinal locations from the vessel. Percent cover by species was estimated via direct vertical observation of the seagrass canopy *in situ* using a 0.25 m^2 quadrat framer subdivided into 100 cells. Previous research demonstrated that the probability of achieving a bias is less than 5% of the overall mean when using only four subsamples (Neckles et al. 2011).

Plant Tissue Condition

Seagrass leaf tissue was collected at every station containing a vegetated bottom. After harvesting the plants, tissue samples were immediately placed on ice in sealed whirl-paks and transported to the University of Texas at Austin Marine Science Institute (UTMSI). Leaf tissue samples were dried to a constant weight in a 60 °C oven and homogenized using a mortar and pestle. Subsamples of leaf

tissue were processed at UTMSI for determination of leaf tissue carbon and nitrogen content, C:N, $\delta^{13}C$, and $\delta^{15}N$ (See Appendix A.3). All plant tissue analyses were limited to *Halodule wrightii* and *Thalassia testudinum*, as these species were the most prevalent and widely distributed among sample sites.

Spatial Data Analysis and Interpolation

ArcGIS software (Environmental Systems Research Institute) was used to manage, analyze, and display spatially referenced point samples and interpolate surfaces for all measured parameters. An inverse distance weighted method was used to assign a value to areas (cells) between sampling points. A total of 12 sampling stations were identified from a variable search radius to generate the value for a single unknown output cell (100 m^2). All data interpolation was spatially restricted to the geographic limits of the submerged vegetation map created during the 2004/2007 NOAA Benthic Habitat Assessment.

RESULTS

Galveston Bay

Water Quality

2018. Stations in Galveston Bay (GB) had a depth of 0.82 ± 0.22 m (mean ± standard deviation) and water temperature of 27.51 ± 0.63 °C (Table 1). GB waters were brackish (26.06 ± 2.61; Table 1) and were the second lowest values of all five regions. Higher salinity values were observed on the leeward side of Galveston Island where lower salinities were documented along the northern portion of West Bay and displayed a difference of ~3 compared to the south shore. Mean dissolved oxygen concentrations were 6.42 ± 0.96 mg L^{-1} (Table 1), with lower concentrations near Jamaica Beach (Delehide Cove). GB did not have any stations that displayed hypoxic conditions. The pH of GB was the lowest of all five regions (7.90 ± 0.15; Table 1). Lower pH values typically corresponded with lower dissolved oxygen concentrations.

Water Column Optical Properties

2018. GB stations were characterized by lower water clarity with a mean downward attenuation coefficient (K_d) of 2.19 ± 0.95 m^{-1} (Table 2). GB had the greatest light attenuation of all five regions, however, these values were comparable to San Antonio Bay (SAB). Highest attenuation coefficients (maximum of 4.56 m^{-1}) were documented in West Bay. Average water column chlorophyll concentrations were 8.6 ± 3.2 µg L^{-1} (Table 2) and greatest near Jamaica Beach (up to 18.6 µg L^{-1}). Highest chlorophyll concentrations typically corresponded with areas of high light attenuation. Mean secchi depth and variability (0.59 ± 0.17 m; Table 2) were the lowest in all five regions. On average, visibility at most stations was poor to fair (within 20 cm of the vegetated or sediment surface). We would like to note that we did not obtain TSS samples for GB in 2018.

Seagrass Coverage and Species Distributions

2018. Approximately 39.9 ± 37.1% of the GB region was devoid of vegetation. The seagrass assemblage in GB was largely dominated by *Halodule wrightii* (51.8 ± 33.7%; Table 3, Figure 4a), followed by *Ruppia maritima* (5.8 ± 9.8%; Table 3, Figure 8a), and *Halophila engelmannii* (2.5 ± 6.9%; Table 3, Figure 7a). Only GB, SAB, and Upper Laguna Madre (ULM) regions were characterized with *H. wrightii* cover greater than 50%. *R. maritima* coverage was highest in GB when compared to the other four regions. Seagrass coverage was lowest near Jamaica Beach, and higher in Christmas Bay and along the north shore of West Bay. Six sampling stations were devoid of seagrass. We would like to note that *T. testudinum* was documented in Christmas Bay in 2016, however, was absent at the sampling stations in 2018. *H. wrightii* canopy height was greatest (16.4 ± 6.4 cm; Table 4), followed by *R. maritima* (14.1 ± 6.1 cm; Table 4), and *H. engelmannii* (6.5 ± 1.7 cm; Table 4). In GB, seagrass canopy height decreased with increasing depth from shore.

Elemental Tissue Composition

2018. H. wrightii C:N molar ratio was 17.7 ± 1.5 (Table 5). Mean $\delta^{13}C$ for *H. wrightii* was -12.9 ± 0.9‰ (Table 5). $\delta^{15}N$ was 4.0 ± 1.7‰ (Table 5; Figure 10), and was the highest value of all five regions with the most enriched values (7.4‰) along the north shore of West Bay.

San Antonio Bay

Water Quality

2018. Stations within San Antonio Bay (SAB) had a depth of 0.86 ± 0.23 m (mean ± standard deviation; Figure 6) and mean water temperature of 27.45 ± 0.66 °C (Table 1). Stations along north Espiritu Santo Bay (behind Blackberry, Dewberry and Long Islands) were shallower (< 1.0 m) than those located on the south side of the bay (backside of Matagorda Island). Salinity values in SAB were brackish (23.95 ± 3.51; Table 1, Figure 7). Mean dissolved oxygen concentrations were 7.85 ± 1.64 mg L^{-1} (Table 1, Figure 8) and higher in north Espiritu Santo Bay (behind Blackberry, Dewberry and Long Islands) than stations located along the south side of the bay. The pH of SAB was the highest of all five regions (8.29 ± 0.23; Table 1, Figure 9) which corresponded with stations that had increased dissolved oxygen concentrations.

Water Column Optical Properties

2018. SAB stations were characterized by lower water clarity with a mean downward attenuation coefficient (K_d) of 2.11 ± 1.40 m^{-1} (Table 2, Figure 10). Light attenuation was comparable to GB but higher than the Coastal Bend (CB), Upper Laguna Madre (ULM) and Lower Laguna Madre (LLM). Light attenuation was high at the majority of sampling stations in SAB. Average water column chlorophyll and TSS concentrations were 7.2 ± 2.9 µg L^{-1} (Table 2, Figure 11) and 23.5 ± 19.9 mg L^{-1} (Table 2, Figure 12), respectively. TSS and chlorophyll concentrations were high behind Matagorda Island, particularly west of Pringle Lake and at some stations within the lake. Mean secchi depth was low (0.66 ± 0.20 m; Table 2) in SAB, especially at stations with highest light attenuation (up to 6.02 m^{-1}). Visibility at most stations was approximately 78% of the water column or within 17 cm of the vegetated or sediment surface, on average.

Seagrass Coverage and Species Distributions

2018. The seagrass assemblage in SAB was dominated by *Halodule wrightii* (50.8 ± 40.2%; Table 3, Figure 13), was devoid of *Thalassia testudinum* (Table 3, Figure 14) and *Syringodium filiforme* (Table 3, Figure 15), but had minimal coverage of *Ruppia maritima* (5.2 ± 13.8%; Table 3, Figure 16) and *Halophila engelmannii* (1.0 ± 3.6%; Table 3, Figure 17). Only GB, SAB, and Upper Laguna Madre (ULM)

regions were characterized with *H. wrightii* cover greater than 50%. Nine sampling stations were documented as 100% bare. Approximately 41.3 ± 38.3% of the SAB region is devoid of vegetation (Table 3, Figure 18). *H. wrightii* canopy height was greatest (22.7 ± 5.9 cm; Table 4), followed by *R. maritima* (16.9 ± 5.2 cm; Table 4), and *H. engelmannii* (6.6 ± 2.0 cm; Table 4). Tallest *H. wrightii* canopy height were observed behind Long Island and west of Pringle Lake.

Elemental Tissue Composition

2018. H. wrightii C:N molar ratio was 18.3 ± 2.6 (Table 5). Mean $\delta^{13}C$ and $\delta^{15}N$ for *H. wrightii* were -12.7 ± 1.5‰ and 0.6 ± 2.3‰, respectively (Table 5; Figure 10). $\delta^{13}C$ values were similar to GB and CB (more depleted), however, $\delta^{15}N$ signatures were the lowest of all regions. The most enriched values (4.0‰) in SAB were observed near Matagorda Bay (Bayucos Island).

Coastal Bend

Water Quality

2017. Stations within the CB had a depth of 0.66 ± 0.24 m (mean ± standard deviation; Figure 6) and mean water temperature of 30.95 ± 2.88 °C (Table 1). Salinity values were hypersaline (37.85 ± 4.90; Table 1, Figure 7), with highest salinities observed along the leeward side of Mustang Island and within Harbor Island. Mean dissolved oxygen concentrations were 5.54 ± 2.53 mg L^{-1} (Table 1, Figure 8). Highest dissolved oxygen concentrations (> 10 mg L^{-1}) were documented behind Traylor and Shellbank Islands, and at some stations near Ransom Point. Four stations experienced hypoxic conditions (< 2 mg L^{-1}) during sampling which were located in East Flats. pH values were high (8.36 ± 0.31; Table 1, Figure 9) and greatest in southern Redfish Bay, Shamrock Cove, and north of Packery Channel behind Padre Island.

2018. Mean water depth (0.80 ± 0.26 m; Figure 6) increased from 2017, however, water temperatures (29.95 ± 1.50 °C) were similar (Table 1). Salinities were variable across sampling stations in the CB region, with a mean of 27.15 ± 7.51 (Table 1, Figure 7). Mean salinities decreased ~10.7 from 2017 to 2018. The CB region displayed a wide range of salinities from 4.68 (Copano and Aransas Bays) to 45.18 (Corpus Christi Bay). Dissolved oxygen concentrations in the CB region

were 6.58 ± 2.03 mg L^{-1} (Table 1, Figure 8). Highest dissolved oxygen concentrations were observed in east Redfish Bay and along the backside of Mustang Island. CB did not have any stations that exhibited hypoxic conditions. pH values were lowest in East Flats and near the Corpus Christi Naval Air Station. Mean pH values for CB were 8.14 ± 0.28 and decreased ~0.25 from 2017 (Table 1, Figure 9).

Water Column Optical Properties

2017. CB stations were characterized by moderate water clarity with a mean downward attenuation coefficient (K_d) of 1.04 ± 0.36 m^{-1} (Table 2, Figure 10). Light attenuation was greatest (~2.0 m^{-1}) in east CB, near Shellbank and Harbor Islands. Average water column chlorophyll and TSS concentrations were 5.0 ± 3.5 µg L^{-1} (Table 2, Figure 11) and 11.7 ± 7.4 mg L^{-1} (Table 2, Figure 12), respectively. Higher TSS concentrations were recorded behind San Jose Island and Padre Island by Packery Channel. Water column chlorophyll concentrations were patchy but had highest concentrations behind San Jose Island and in Redfish Bay. Mean secchi depth was variable (0.63 ± 0.21 m; Table 2) with visibility at most stations near the entire depth of the water column or within 3 cm of the vegetated or sediment surface, on average.

2018. The mean downward attenuation coefficient (K_d) and variability increased (1.32 ± 0.69 m^{-1}; Table 2, Figure 10) since sampling in 2017. High light attenuation was patchy, with greatest light attenuation in Copano and Nueces Bays, northern Redfish Bay, and on the backside of Mustang Island (Aransas Bay). Generally, the highest attenuation values were recorded in locations with greater water column chlorophyll (4.3 ± 3.3 µg L^{-1}; Table 2, Figure 11) or TSS (7.8 ± 6.1 mg L^{-1}; Table 2, Figure 12) concentrations. High water column chlorophyll concentrations were documented in Aransas Bay and patches along the west side of Redfish Bay. However, TSS concentrations were low with the exception of few stations near Shamrock Island. Although light attenuation was higher in 2018 than in 2017, mean secchi depth increased (0.72 ± 0.25 m; Table 2), and visibility was within 8 cm of the vegetated or sediment surface, on average.

Seagrass Coverage and Species Distributions

2017. The seagrass assemblage in CB was dominated by *Halodule wrightii* (33.7 ± 39.0%; Table 3, Figure 13), followed by *Thalassia testudinum* (25.1 ± 36.8 %; Table 3, Figure 14), *Syringodium filiforme* (5.9 ± 16.6%; Table 3, Figure 15),

Ruppia maritima (1.0 ± 4.1%; Table 3, Figure 16) and *Halophila engelmannii* (0.3 ± 1.6%; Table 3, Figure 17). Approximately 33.9 ± 32.7% of the CB region is devoid of vegetation, with six sampling stations documented as 100% bare (Table 3, Figure 18). Lower seagrass coverage was observed in Aransas Bay (backside of San Jose Island), Redfish Bay (near Dagger, Stedman, and Traylor Islands), and near Shamrock Cove. *H. wrightii* coverage was widely distributed, except for minor coverage along the west side of Redfish Bay. At stations in west Redfish Bay, meadows were dominated with *T. testudinum* but did include some patchy bare or low coverage areas near Stedman and Traylor Islands. The CB region had minimal coverage of *R. maritima*, *H. engelmannii*, and *S. filiforme*. *T. testudinum* canopy height was greatest (34.3 ± 9.1 cm; Table 4), followed by *S. filiforme* (23.9 ± 7.8 cm; Table 4), *H. wrightii* (18.0 ± 4.5 cm; Table 4), *R. maritima* (13.2 ± 5.9 cm; Table 4), and *H. engelmannii* (5.6 ± 2.0 cm; Table 4). The average canopy height was tall, particularly in Redfish Bay.

2018. Total seagrass coverage in the CB region was 71.7 ± 30.6%. The seagrass assemblage in CB was dominated again by *H. wrightii* (37.6 ± 41.4%; Table 3, Figure 13), followed by *T. testudinum* (24.2 ± 35.3%; Table 3, Figure 14), *S. filiforme* (8.1 ± 19.7%; Table 3, Figure 15), *R. maritima* (0.8 ± 4.6%; Table 3, Figure 16), and *H. engelmannii* (1.0 ± 5.0%; Table 3, Figure 17). Approximately 28.3 ± 30.6% of the CB region was bare, which consisted of five sampling stations completely devoid of seagrass (Table 3, Figure 18). Spatial distributions were similar to 2017, where lower seagrass coverage was observed in Aransas (backside of San Jose Island) and Redfish Bays, specifically near Dagger, Stedman, and Traylor Islands. *H. wrightii* had very little coverage along the west side of Redfish Bay. West Redfish Bay was dominated by *T. testudinum* with some bare or low coverage areas near Stedman and Traylor Islands. However, it should be noted that *H. wrightii* coverage was greatest in east Redfish Bay (on the leeward side of the islands in this area) where *T. testudinum* was largely absent except along the deeper edges of the bay. Lastly, the CB region had minimal coverage of *R. maritima*, *H. engelmannii*, and *S. filiforme*. In comparison to 2017, *T. testudinum*, *R. maritima*, and *H. engelmannii* coverages were similar, however, there was a slight increase in *H. wrightii* (~4%) and *S. filiforme* (~3%) coverage. *T. testudinum* canopy height was tallest (30.4 ± 8.1 cm; Table 4), followed by *S. filiforme* (26.2 ± 8.1 cm; Table 4), *H. wrightii* (17.7 ± 5.6 cm; Table 4), *R. maritima* (12.0 ± 5.4 cm; Table 4), and *H. engelmannii* (5.3 ± 2.1 cm; Table 4). The most notable changes in canopy height was a decrease in *T. testudinum* (~4 cm) and an increase in *S. filiforme* (~3 cm).

Elemental Tissue Composition

2017. H. wrightii C:N molar ratio was 20.0 ± 2.3 (Table 5). Mean $\delta^{13}C$ for *H. wrightii* was -11.9 ± 1.4‰ (Table 5) and $\delta^{15}N$ was 1.3 ± 2.6‰ (Table 5; Figure 10). The most enriched *H. wrightii* $\delta^{15}N$ value (8.5‰) was documented in Nueces Bay near Portland. The mean *T. testudinum* C:N molar ratio (15.3 ± 1.9) was lower than the value reported for *H. wrightii* (Table 5). The mean *T. testudinum* carbon ($\delta^{13}C$) and nitrogen ($\delta^{15}N$) isotope signatures were -10.2 ± 1.1 and 2.9 ± 1.4‰, respectively (Table 5). The maximum *T. testudinum* $\delta^{15}N$ value was 5.9‰ with the most enriched stations in south Redfish Bay. In comparison to the LLM, mean $\delta^{13}C$ values were more depleted yet $\delta^{15}N$ values were more enriched for *T. testudinum.*

2018. H. wrightii C:N molar ratio was 18.2 ± 2.5 which decreased from 2017 (Table 5). Mean $\delta^{13}C$ for *H. wrightii* (-12.1 ± 3.3‰; Table 5) and $\delta^{15}N$ (1.4 ± 2.2‰; Table 5) were similar to 2017 measurements. The most enriched *H. wrightii* $\delta^{15}N$ value (8.9‰) was again observed in Nueces Bay near Portland. *T. testudinum* C:N molar ratio was 15.4 ± 1.7 and lower in CB than LLM (Table 5). Mean *T. testudinum* carbon and nitrogen isotope signatures were -10.2 ± 0.7 ($\delta^{13}C$) and 3.0 ± 1.6‰ ($\delta^{15}N$), respectively (Table 5). The maximum *T. testudinum* $\delta^{15}N$ value was 6.3‰ and most enriched stations (5.0 to 6.3‰) were again observed in west Redfish Bay near Aransas Pass and Ingleside. Means and variability for C:N, $\delta^{13}C$, and $\delta^{15}N$ for *T. testudinum* were similar in comparison to 2017.

Upper Laguna Madre

Water Quality

2017. The ULM region had a depth of 1.04 ± 0.52 m (mean ± standard deviation; Figure 6) and an average water temperature of 29.25 ± 3.92 °C (Table 1). Water depth (> 1.60 m) was highest along the west side of ULM. Average daily water temperatures displayed seasonal patterns that ranged from 8 °C (January) to 33 °C (August; Figure 3) at Bird Island. At Nine Mile Hole, temperatures displayed drastic temperature changes (particularly during winter) and ranged from 6 °C (January) to 32 °C (August; Figure 4). Hypersaline conditions (41.52 ± 5.54; Table 1, Figure 7) where characteristic of this region, where salinities exceeded 40 along the east side of ULM, north of Bird Island. Additionally, higher salinities were found

outside Flour Bluff and at some stations south of Baffin Bay to Nine Mile Hole. Reduced salinities typically corresponded with greater water column depths along the west side of ULM, south of Flour Bluff. In the ULM region, salinities exceeded 40 at approximately 1.10 m in depth. Mean daily salinity measurements from HOBO loggers deployed near Bird Island showed that salinities fluctuated between 34–52 (January–December 2017; Figure 3). Continuous mean daily salinity measurements from HOBO loggers deployed in Nine Mile Hole displayed similar fluctuations in salinity, exhibiting a range of 42–53 in 2017 (Figure 4). ULM had high dissolved oxygen concentrations (5.89 ± 1.48 mg L^{-1}; Table 1, Figure 8) and no stations exhibited hypoxic conditions. Highest dissolved oxygen concentrations were observed near Flour Bluff, Bird Island, and Baffin Bay. The ULM region had a mean pH of 8.32 ± 0.24 (Table 1, Figure 9), with greatest values (> 9.00) documented south of Baffin Bay to Nine Mile Hole.

2018. Stations in the ULM region had a greater depth (1.11 ± 0.47 m; Table 1, Figure 6) but cooler mean water temperature (26.95 ± 3.58 °C; Table 1). Salinities decreased from ~42 to 33.74 ± 1.47 (Table 1, Figure 7). Salinities were low across the majority of the region with the exception of stations located on the east side of the bay (north of Packery Channel). Continuous mean daily salinity measurements near Bird Island showed fluctuations (40–50) in salinity in January 2018, followed by a decline by April (~25). Salinities increased slightly (up to ~35) which declined to 20 by December 2018 (Figure 3). HOBO mean daily salinity measurements in Nine Mile Hole showed salinities of 40–50 until June, a decline to 15 in late June, and an increase to 40 by end of August 2018 (Figure 4). ULM had a mean dissolved oxygen concentration of 6.33 ± 1.31 mg L^{-1} (Table 1, Figure 8), which increased slightly from 2017. The highest dissolved oxygen concentrations were observed near Middle Ground. ULM had a mean pH of 8.07 ± 0.20 (Table 1, Figure 9) which decreased by about 0.25 from 2017. pH values were highest in the southern part of the region, from Middle Ground south to Nine Mile Hole and the Land Cut.

Water Column Optical Properties

2017. Mean K_d was 1.16 ± 0.59 m^{-1} (Table 2, Figure 10) and highest in the ULM compared to the CB and LLM regions. High light attenuation values were recorded throughout much of ULM, where greatest attenuation occurred in areas of higher water column chlorophyll or TSS concentrations. Mean water column chlorophyll and TSS concentrations were 3.8 ± 3.3 µg L^{-1} (Table 2, Figure 11) and 15.9 ± 13.1 mg L^{-1} (Table 2, Figure 12), respectively. Highest water column chlorophyll concentrations (> 10 µg L^{-1}) were patchy and observed near the JFK Causeway

south to Pita Island, and included much of Nine Mile Hole. Greatest TSS concentrations were documented in Nine Mile Hole which corresponded with shallower water depths. Secchi depth had the greatest variability (1.00 ± 0.52 m; Table 2) of all three regions likely attributed to the patchy distribution of TSS and chlorophyll concentrations. Water transparency was approximately 50% of the water column, on average.

2018. The ULM stations exhibited a K_d of 1.45 ± 0.61 m^{-1} (Table 2, Figure 10), which increased from 2017 observations. Although higher light attenuation values were patchy, these values covered much of the region. Stations with high attenuation generally coincided with increased concentrations of water column chlorophyll, TSS, or both. Water column chlorophyll concentration (4.8 ± 2.4 µg L^{-1}; Table 2, Figure 11) increased but TSS concentrations (11.5 ± 14.6 mg L^{-1}; Table 2, Figure 12) decreased from 2017. Higher TSS concentrations were patchy and observed near the mouth of Baffin Bay and south to the Land Cut. Whereas higher chlorophyll concentrations were also patchy and documented at the mouth of Baffin Bay, but extended north. Mean secchi depth was similar to 2017 (0.96 ± 0.42 m; Table 2) measurements. At most stations, visibility was ~15 cm of the vegetated or sediment surface, on average.

Seagrass Coverage and Species Distributions

2017. H. wrightii (60.1 ± 36.6%; Table 3, Figure 13) dominated the region, followed by *S. filiforme* (6.2 ± 16.2%; Table 3, Figure 15), and *H. engelmannii* (0.2 ± 1.4%; Table 3, Figure 17). The ULM was devoid of *T. testudinum* and *R. maritima*. Bare substrate covered 33.5 ± 35.3% (Table 3, Figure 18) of the ULM region. Eighteen sampling stations in this region did not have vegetation present and approximately 27% of these stations were located in Nine Mile Hole. The other remaining stations were scattered throughout the ULM but corresponded with greater water depths (1.5 to 2.5 m). Seagrass coverage was lowest in the southern portion of ULM from Middle Ground south to Nine Mile Hole and the Land Cut. Other bare areas included the mouth of Baffin Bay and patches in central ULM where water depths were greater. *H. wrightii*, the dominant species, was found throughout ULM but was largely absent in Nine Mile Hole, north of the JFK Causeway, and in some areas along the western side of the ULM. Furthermore, some areas west of the ICW in central ULM experienced a loss in *S. filiforme* with minimal recolonization by *H. wrightii* in 2014 due to severe drought conditions. Interestingly, modest *S. filiforme* coverage was found north of JFK Causeway and in some areas along the western side of the ULM. It appears that *S. filiforme* may be slowly recolonizing the areas it previously occupied. Areas that were bare or had low seagrass cover,

where depth was < 1.0 m), typically corresponded with high TSS concentrations and light attenuation. These conditions likely impaired conditions for seagrass growth and colonization. *S. filiforme* canopy height was tallest (22.8 ± 6.8 cm; Table 4), followed by *H. wrightii* (20.8 ± 7.0 cm; Table 4), and *H. engelmannii* (7.2 ± 1.4 cm; Table 4). *H. wrightii* mean canopy height was greatest in the ULM region.

2018. The seagrass assemblage was again dominated by *H. wrightii* (56.0 ± 35.8%; Table 3, Figure 13), followed by *S. filiforme* (9.2 ± 20.6%; Table 3, Figure 15), and *H. engelmannii* (0.5 ± 2.8%; Table 3, Figure 17). *R. maritima* and *T. testudinum* were absent from this region. Bare substrate covered 34.2 ± 34.8% (Table 3, Figure 18) of the ULM region. Only six sampling stations had no vegetation present, which was a 60% reduction in the number of the bare sampling stations observed in 2017. Seagrass coverage was lowest in the southern portion of ULM, south of Baffin Bay to the Land Cut, and at stations that had the deepest depth measurements. *H. wrightii* was found throughout ULM, but was largely absent outside of the Corpus Christi Naval Air Station and Baffin Bay. Although total coverage remained similar to 2017, there was a change in species composition as *H. wrightii* coverage decreased slightly (~4%) but *S. filiforme* increased (~3%). *S. filiforme* canopy height was again tallest (26.8 ± 6.9 cm; Table 4), followed by *H. wrightii* (20.4 ± 7.6 cm; Table 4), *H. engelmannii* (6.6 ± 2.2 cm; Table 4), and *R. maritima* (5.2 ± 0 cm; Table 4). *H. wrightii* canopy height did not change between 2017 and 2018, however, *S. filiforme* canopy height increased ~4 cm. Tallest H. wrightii was observed north of Baffin Bay.

Elemental Tissue Composition

2017. H. wrightii C:N molar ratio was 20.7 ± 2.7 (Table 5), with a minimum and maximum ratio of 14.4 and 28.0, respectively. Mean *H. wrightii* carbon and nitrogen isotope signatures were -12.1 ± 1.5 ‰ ($\delta^{13}C$) and 2.5 ± 1.3‰ ($\delta^{15}N$), respectively (Table 5). The maximum *H. wrightii* $\delta^{15}N$ signature was 4.6 ‰ which was the least enriched value of all three regions.

2018. The *H. wrightii* C:N molar ratio was 17.2 ± 2.1 (Table 5), with a minimum and maximum ratio of 16.1 and 27.0, respectively. *H. wrightii* C:N decreased from 2017. Mean C:N ratios were relatively consistent throughout ULM. Mean *H. wrightii* carbon and nitrogen isotope signatures were -14.4 ± 1.2 ($\delta^{13}C$) and 2.9 ± 1.7‰ ($\delta^{15}N$), respectively (Table 5). $\delta^{13}C$ values were more depleted in 2018 than in 2017, however, $\delta^{15}N$ values were similar.

Lower Laguna Madre

Water Quality

2017. LLM stations exhibited a depth of 0.89 ± 0.37 m (Table 1, Figure 6) and a mean water temperature of 22.53 ± 3.24 °C (Table 1). Continuous daily mean measurements of water temperature exhibited seasonal patterns, ranging from 7 °C (January) to 31 °C (June; Figure 5). Greatest water depths were observed in the southernmost area of LLM near South Padre Island and Laguna Vista. Mean salinities in this region were 38.80 ± 4.42 (Table 1, Figure 7). Highest salinities were observed in the northernmost area of LLM from the Land Cut south to Port Mansfield. The lowest salinities (~30) were documented near the mouth of the Arroyo Colorado River and extended northward to Port Mansfield. Continuous salinity data observations in southern LLM (near South Padre Island) showed relatively stable conditions (30–40) from March 2016 to November 2017 (Figure 5). We would like to note that from June to November 2017, the HOBO conductivity logger failed so temperature and salinity values were removed. Mean dissolved oxygen concentration in LLM was 7.74 ± 1.71 mg L^{-1} (Table 1, Figure 8). No stations revealed hypoxic conditions during sampling. The highest dissolved oxygen concentrations were found outside the mouth of the Arroyo Colorado River and near La Punta Larga. Mean pH values for the LLM region were 8.13 ± 0.19 (Table 1, Figure 9) and were greatest where highest dissolved oxygen concentrations were observed.

2018. Mean water depth (0.85 ± 0.34 m; Table 1, Figure 6) in LLM was similar to 2017, however, water temperatures were cooler (17.71 ± 3.80 °C; Table 1). Cooler water temperatures were a result of cold fronts and sampling time (late November). Continuous daily mean water temperature measurements exhibited seasonal patterns, ranging from 4 °C (January) to 29 °C (June; Figure 5). Greatest water depths were observed in northern and southern LLM. In comparison to 2017, salinity measurements decreased (~9) and were relatively stable, exhibiting little variability (30.30 ± 2.35; Table 1, Figure 7) throughout the entire region. Highest salinity values (up to 43) were observed in South Bay and lowest values (20) were observed north of the mouth of the Arroyo Colorado River. Continuous HOBO measurements showed that salinities decreased slightly from ~35 (November 2017) to ~25 by April 2018. By June 2018, salinities increased to 32 (Figure 5). Dissolved oxygen concentrations in the LLM region were similar but had greater variability when compared to 2017 (7.60 ± 2.03 mg L^{-1}; Table 1, Figure 8). Lowest and highest dissolved oxygen concentrations were found north of Port Mansfield

and south of the Arroyo Colorado River, respectively. Mean pH values for LLM were 8.20 ± 0.21 (Table 1, Figure 9).

Water Column Optical Properties

2017. Mean K_d was 1.00 ± 0.50 m^{-1} (Table 2, Figure 10) across the LLM stations. Light attenuation was similar to the CB region and less than the ULM. However, variability was greater than CB and comparable to ULM. Highest light attenuation values were observed outside of the Laguna Atascosa. Water column chlorophyll (1.3 ± 1.5 µg L^{-1}; Table 2, Figure 11) were low in concentration and displayed little variability compared to CB and ULM. TSS concentrations (8.1 ± 6.8 mg L^{-1}; Table 2, Figure 12) were lowest in LLM in comparison to the other two regions, where greater concentrations were generally restricted to the Laguna Atascosa. Although secchi depth displayed some variability (0.80 ± 0.31 m; Table 2), water transparency was high at most stations. Visibility was near the entire depth of the water column and water transparency was greatest in the LLM region.

2018. Mean K_d (0.99 ± 0.51 m^{-1}; Table 2, Figure 10) was nearly identical to the downward attenuation coefficient observed in 2017. Light attenuation in LLM was patchy, with higher light attenuation values north of the Arroyo Colorado River to the Land Cut and near the Laguna Atascosa National Wildlife Refuge. Water column chlorophyll concentrations increased slightly from 2017 (3.3 ± 3.3 µg L^{-1}; Table 2, Figure 11) but mean total suspended solids were similar (8.2 ± 8.9 mg L^{-1}; Table 2, Figure 12). Secchi depth and variability were nearly identical to 2017 measurements (0.83 ± 0.33 m; Table 2) with high water clarity particularly in the southern area of the region. At most stations, visibility was near the entire depth of the water column or within 2 cm of the vegetated or sediment surface.

Seagrass Coverage and Species Distributions

2017. H. wrightii dominated the seagrass assemblage in LLM (34.2 ± 38.1%; Table 3, Figure 13), followed by *T. testudinum (*24.1 ± 32.9%; Table 3, Figure 14*), S. filiforme* (2.2 ± 9.8%; Table 3, Figure 15) and *H. engelmannii* (1.4 ± 7.3%; Table 3, Figure 17). At the stations sampled, *R. maritima* was absent in this region. Approximately 38.0 ± 34.5% of LLM was bare (Table 3, Figure 18). Thirteen sampling stations in this region had no vegetation present, however, a large number of stations were documented to contain < 5 % coverage. Seagrasses were largely absent outside of the Laguna Atascosa south to Laguna Vista (west of the spoil islands). From the northernmost section of LLM to just south of the Arroyo

Colorado River outside of the Laguna Atascosa National Wildlife Refuge, *H. wrightii* was the dominant species. Greatest coverage of *H. wrightii* was observed to the north (to Port Mansfield) and south (to Laguna Atascosa National Wildlife Refuge) of the mouth of the Arroyo Colorado River. The presence of *T. testudinum* was confined to the southernmost region of LLM and just outside the Laguna Atascosa. *S. filiforme* (18.5 ± 6.7 cm; Table 4) and *T. testudinum* (18.5 ± 5.4 cm; Table 4) canopy height were tallest, followed by *H. wrightii* (15.6 ± 6.0 cm; Table 4), and *H. engelmannii* (5.6 ± 1.7 cm; Table 4). Mean canopy height was shortest in LLM compared to the ULM and CB regions.

2018. H. wrightii dominated the seagrass assemblage in LLM (31.6 ± 34.9%; Table 3, Figure 13), followed by *T. testudinum (*23.8 ± 32.3%; Table 3, Figure 14*), S. filiforme* (2.4 ± 9.5%; Table 3, Figure 15), *H. engelmannii* (0.5 ± 2.6%; Table 3, Figure 17), and negligible presence of *R. maritima* (0 ± 0.1%; Table 3, Figure 16). Mean bare coverage increased from 38% in 2017 to 41.6 ± 31.8% in 2018 (Table 3, Figure 18). Eleven sampling stations in this region were devoid of vegetation. Seagrasses were absent along the eastern side of LLM, north of La Punta Larga behind Padre Island, and east of the spoil islands from Stover Point south to Laguna Vista. *H. wrightii* dominated from the northernmost area of LLM to Stover Point. From south of this area, *T. testudinum* coverage dominated to South Padre Island. In comparison to 2017, mean *T. testudinum* coverage was similar but there was a slight increase in *H. wrightii* (~3%). *S. filiforme* canopy height remained tallest (24.9 ± 7.3 cm; Table 4), followed by *T. testudinum* (19.2 ± 6.9 cm; Table 4), *R. maritima* (11.9 ± 3.3 cm; Table 4), *H. wrightii* (13.5 ± 5.9 cm; Table 4), and *H. engelmannii* (5.1 ± 1.5 cm; Table 4). The greatest difference in mean canopy height between 2017 and 2018 was observed in *S. filiforme* and *R. maritima* (increase in ~6 and 12 cm, respectively).

Elemental Tissue Composition

2017. Mean C:N molar ratio for *H. wrightii* was 18.0 ± 1.8 and the lowest of all three regions (Table 5). $\delta^{13}C$ and $\delta^{15}N$ signatures for *H. wrightii* were -9.9 ± 1.4‰ and 3.2 ± 2.4‰, respectively (Table 5). The maximum *H. wrightii* $\delta^{15}N$ value in LLM was 13.5‰, where enriched $\delta^{15}N$ signatures were found north and south of the mouth of the Arroyo Colorado River. *T. testudinum* C:N molar ratio (16.5 ± 2.5) was higher in LLM than CB (Table 5). Mean *T. testudinum* $\delta^{13}C$ was similar to CB (-9.5 ± 1.0‰) but differed in mean $\delta^{15}N$ (2.2 ± 1.7‰; Table 5). The maximum *T. testudinum* $\delta^{15}N$ value in LLM was 5.3‰, north of Port Isabel.

2018. The mean C:N molar ratio for *H. wrightii* was 19.4 ± 2.7 and the highest of all five regions (Table 5). $\delta^{13}C$ and $\delta^{15}N$ signatures for *H. wrightii* were -10.9 ± 1.8‰ and 3.4 ± 2.4‰, respectively (Table 5). The maximum *H. wrightii* $\delta^{15}N$ value in LLM was 9.6‰, near Chubby Island. Enriched $\delta^{15}N$ signatures were found near the Arroyo Colorado River and extended northward. *T. testudinum* C:N molar ratio increased from 2017 to 18.0 ± 2.6 (Table 5). Mean *T. testudinum* $\delta^{13}C$ (-9.9 ± 1.8) and $\delta^{15}N$ (2.3 ± 1.7‰) signatures were similar to 2017 (Table 5). Variabilities in C:N, $\delta^{13}C$, and $\delta^{15}N$ of *T. testudinum* were nearly identical (difference of 0.1) with the exception of $\delta^{13}C$ values (difference of 0.4). The maximum *T. testudinum* $\delta^{15}N$ value in LLM was 6.0‰ near Stover Point. The second highest value of 5.6‰ was observed north of Port Isabel near the ICW, the same station that documented enriched $\delta^{15}N$ values in 2017.

DISCUSSION

Galveston Bay

Salinity values ranged from 19–30, with higher salinities on the leeward side of Galveston Island and lower salinities (difference of ~3) along the north shore of West Bay. Monthly rainfall was above normal from mid-September to December 2018 which explains the salinity gradient observed in the GB region. Salinity values increased from Galveston Bay proper to San Luis Pass. The pH of GB was the lowest of all five regions (7.90) and lower pH values typically corresponded with lower dissolved oxygen concentrations. In addition, lower salinity values may have also contributed to lower pH values. GB had the greatest light attenuation and chlorophyll concentrations of all five regions. Stations characterized by high light attenuations in the GB region correlated to areas with increased water column chlorophyll concentrations. Despite higher light attenuation, $\delta^{13}C$ values (-14.4‰ to -10.2‰) do not immediately suggest light limitation. The maximum *H. wrightii* $\delta^{15}N$ (7.4‰) signature, observed near Jamaica Beach, was the third highest value of all five regions and suggests anthropogenic input. Despite decreased water transparency, seagrass coverage was moderate to high across stations. *R. maritima* coverage was highest in GB when compared to the other four regions. *H. wrightii* coverage (~52%) was the second highest of all five regions with only a mean of 40% bare coverage. Seagrass coverage was lowest near Jamaica Beach, and higher in Christmas Bay and along the north shore of West Bay. Although we did not document *T. testudinum* at our stations in Christmas Bay in 2018, it has been present in previous years (pers. comm., P. Bohannon). In the GB region,

seagrass canopy height decreased with increasing depth from shore. Overall, the mixed assemblage of seagrasses covered approximately 60% of the bay floor in GB and communities appear to be relatively stable.

San Antonio Bay

Salinity values in SAB were brackish and ranged from 11–30 which was comparable to the GB region. Similar to GB, monthly rainfalls were above normal from mid-September to October 2018. SAB stations were characterized by lower water clarity and had the second highest light attenuation values of all five regions (comparable to GB). Stations characterized by high light attenuations in the SAB region correlated to areas of higher water column chlorophyll or TSS concentrations. SAB ranked second highest for water column chlorophyll and highest of all five regions for TSS concentrations. The pH was highest in SAB which corresponded with stations that had increased dissolved oxygen concentrations. *H. wrightii* $\delta^{13}C$ values ranged from -16.1‰ to -10.5‰, where more depleted values (-16.1‰) could possibly suggest either decreased light availability or a dissolved inorganic carbon source. The maximum *H. wrightii* $\delta^{15}N$ (4.0‰) signature, observed near Matagorda Bay, was the lowest of all five regions and do not immediately suggest any major anthropogenic inputs into SAB. The seagrass composition was similar to the GB region, with *H. wrightii* (51%) as the dominant seagrass followed by R. maritima with 5% coverage. SAB region was one of three regions that had *H. wrightii* cover greater than 50%. Overall, the assemblage of seagrasses covered approximately 57% of the bay floor in SAB.

Coastal Bend

Mean water depth increased approximately ~20 cm while salinities decreased ~11 from 2017 to 2018. In 2017, salinities were hypersaline with highest salinities observed in Corpus Christi Bay. By 2018 sampling, the CB region displayed a wide range of salinities from 5 (Copano and Aransas Bays) to 45 (Corpus Christi Bay). Monthly rainfalls were above normal in 2018, explaining the salinity gradient in this region. In general, the highest attenuation values were recorded in locations with greater water column chlorophyll or TSS concentrations, where the light attenuation coefficient increased from 2017 to 2018. Spatial distributions were similar to 2017, where lower seagrass coverage was observed in Aransas (backside of San Jose Island) and Redfish Bays, specifically near Dagger,

Stedman, and Traylor Islands. West Redfish Bay was dominated by *T. testudinum* with some bare or low coverage areas near Stedman and Traylor Islands. These areas of low seagrass cover were impacted by Hurricane Harvey on 26 August 2017. We documented substantial declines in *T. testudinum* relative to *H. wrightii* in Redfish Bay and recovery has yet to return to pre-storm coverage values in some areas (Congdon et al. 2019). In 2017 and 2018, *H. wrightii* had very little coverage along the west side of Redfish Bay. It is likely that *T. testudinum* populations were excluding *H. wrightii* from expanding into this area. However, it should be noted that *H. wrightii* coverage was greatest in east Redfish Bay (on the leeward side of the islands in this area) where *T. testudinum* was largely absent with the exception of deeper edges of the bay. Therefore, water depth was likely influencing these spatial distributions of *H. wrightii* and *T. testudinum*. Lastly, the CB region had minimal coverage of *R. maritima*, *H. engelmannii*, and *S. filiforme*. In comparison to 2017, *T. testudinum*, *R. maritima*, and *H. engelmannii* coverages were similar, however, there was a slight increase in *H. wrightii* (~4%) and *S. filiforme* (~3%) coverage. The most notable changes in canopy height was a decrease in *T. testudinum* (~4 cm) and an increase in *S. filiforme* (~3 cm). Reductions in the canopy height of *T. testudinum* likely reflect the slow recovery from Hurricane Harvey as we had observed an immediate decline in blade lengths due to ripped and removed blades (Congdon et al. 2019). Overall, seagrasses covered approximately 72% of the bay floor in CB which was the highest of all five regions. *H. wrightii* C:N molar ratio decreased from 2017 but mean $\delta^{13}C$ and $\delta^{15}N$ signatures were similar to 2017 measurements. In both years, the most enriched *H. wrightii* $\delta^{15}N$ value (8.9‰) was observed in Nueces Bay near Portland. Means and variability for C:N, $\delta^{13}C$, and $\delta^{15}N$ for *T. testudinum* were similar in comparison to 2017. The maximum *T. testudinum* $\delta^{15}N$ value was 6.3‰ and most enriched stations (5.0 to 6.3‰) were documented in the same location in west Redfish Bay near Aransas Pass and Ingleside for both 2017 and 2018.

Upper Laguna Madre

From 2017 to 2018, water depth in the ULM region increased approximately 7 cm. Near Bird Island, mean daily salinity measurements showed that salinities fluctuated between 35–50 (January 2017 – April 2018). The ULM is restricted from any significant tidal inlet or freshwater sources. As a result, higher salinity values are likely attributed to long water residence times with minimal flushing. By June 2018, salinity measurements declined to ~30 and then to ~20 by December 2018. Most of the region displayed lower salinities than normal in 2018 (~33) which can be explained by above average monthly rainfall was above normal in June,

September. High light attenuation values were recorded throughout much of ULM and increased from 2017, where greatest attenuation occurred in areas of higher water column chlorophyll and TSS concentrations. Areas that were bare or had low seagrass cover, where depth was < 1.0 m), typically corresponded with high TSS concentrations and light attenuation. Water transparency was approximately 50% of the water column, on average. Therefore, it is possible that these conditions likely impaired seagrass growth and colonization. Despite a small decline in water quality conditions, total coverage remained similar to 2017 (< 1% difference). There was a change in species composition as *H. wrightii* coverage decreased slightly (~4%) but *S. filiforme* increased (~3%) between 2017 and 2018. In addition, *S. filiforme* canopy height increased ~4 cm during this time. The increase in *S. filiforme* coverage occurred to the north and south of the JFK Causeway. *S. filiforme* populations have been slowly recovering to pre-drought conditions since the massive loss of *S. filiforme* in 2014 due to hypersaline conditions (Wilson and Dunton 2017). *H. wrightii* C:N decreased from 2017. $\delta^{13}C$ values were more depleted in 2018 than in 2017, however, $\delta^{15}N$ values were similar. In both years, the maximum *H. wrightii* $\delta^{15}N$ signatures (~5‰) were observed outside and to the south of Baffin Bay. Therefore, it is possible that higher values in *H. wrightii* tissue reflect freshwater run-off into the ULM region.

Lower Laguna Madre

In comparison to 2017, salinity measurements decreased (~9) and were relatively stable, displaying minor variability throughout the entire region. In 2017, hypersaline conditions were observed in the northernmost area of LLM from the Land Cut south to Port Mansfield. The lowest salinities (~30) were documented near the mouth of the Arroyo Colorado River and extended northward to Port Mansfield. However, in 2018, highest salinity values (up to 43) were observed in South Bay and lowest values (~20) were observed north of the mouth of the Arroyo Colorado River. The change in mean salinity between 2017 and 2018 is largely a result of higher than normal precipitation occurring in south Texas (and most of the state). Mean light attenuation was nearly identical to values observed in 2017. In both years, higher light attenuation values were typically documented north of the Arroyo Colorado River and near the Laguna Atascosa National Wildlife Refuge. Despite areas of higher light attenuation, K_d values, water column chlorophyll, and TSS concentrations were the lowest of all five regions. Water transparency was high and visibility was near the entire depth of the water column in the LLM region. *H. wrightii* and *T. testudinum* exhibited similar spatial distributions in 2017 and 2018. *H. wrightii* dominated from the northernmost area of LLM to Stover Point

where, *T. testudinum* coverage dominated south of this point to South Padre Island. In comparison to 2017, mean *T. testudinum* coverage was similar but there was a slight increase in *H. wrightii* (~3%). From 2017 to 2018, the mean C:N molar ratio for *H. wrightii* increased by 1.4. $\delta^{13}C$ and $\delta^{15}N$ signatures for *H. wright* increased by 1.8‰ and 0.2‰, respectively. In 2017, the maximum *H. wrightii* $\delta^{15}N$ value was 13.5‰ and found north and south of the mouth of the Arroyo Colorado River. In 2018, the maximum *H. wrightii* $\delta^{15}N$ value in LLM was 9.6‰ (near Chubby Island) and most enriched $\delta^{15}N$ signatures were found near the Arroyo Colorado River. The patterns in *H. wrightii* $\delta^{15}N$ values from 2017 and 2018 suggest that the Arroyo Colorado River is a major source of anthropogenic input into the LLM region. The mean C:N molar ratio for *T. testudinum* increased by 1.5. $\delta^{13}C$ and $\delta^{15}N$ signatures for *T. testudinum* showed little change from 2017 to 2018 (0.4‰ and 0.1‰, respectively). In 2017, the maximum *T. testudinum* $\delta^{15}N$ value in LLM was 5.3‰, north of Port Isabel. In 2018, the maximum *T. testudinum* $\delta^{15}N$ value in LLM was 6.0‰ near Stover Point. The second highest value of 5.6‰ was observed north of Port Isabel near the ICW, the same station that documented enriched $\delta^{15}N$ values in 2017. Enriched *T. testudinum* $\delta^{15}N$ values from 2017 and 2018 suggest anthropogenic input into the LLM region.

ACKNOWLEDGEMENTS

We thank the amazing staff at the University of Texas Marine Science Institute (UTMSI) for providing logistical support to allow us to sample coastwide over the past two years, including the period following Harvey's landfall despite enormous damage to our institute facilities. In particular, we are indebted to Frank Ernst for providing reliable vessels that helped us to conduct intensive field studies and our colleagues at Texas A&M University–Corpus Christi (Brien Nicolau and Paul Zimba) for providing lab facilities for sample processing. In addition to the funding from the Texas General Land Office and the excellent support from our program manager Julie McEntire (CMP Cycle 22, Contract No. 18-083-000-A592), we are deeply appreciative of continued funding support provided by the Coastal Bend Bays and Estuaries Program (Ray Allen; Contract No. 1610), the National Park Service (Martha Segura; CESU Contract No. P16AC01794), and, with in-kind support from the NOAA funded Mission-Aransas National Estuarine Research Reserve (Jace Tunnell). We thank the numerous people at UTMSI who have supported our Tier 2 field efforts, including our highly experienced field team led by Kim Jackson. Our field and laboratory assistants included Christina Bonsell, Meagan Cuddy, Jason Jenkins, Ashley Moreno, Nick Reyna, and Caitlin Young. Without them the field work would clearly not have been completed. We also acknowledge the support of our faithful partners at TCEQ (Pat Bohannon and Lythia Metzmeier) and TPWD (Cindy Hobson and Faye Grubbs) and their team members (Rodney Adams, Stacey Carr, Elizabeth Kompanik, Laura Ryckman, and Sarah Whitley). Finally, a very special note of sincere thanks to our data manager, Tim Whiteaker (Center for Water and the Environment at UT-Austin), who was absolutely instrumental in developing the GIS maps seen in this report, posting results and updates on our dedicated web page (www.texasseagrass.org), and archiving the data and metadata at NCEI (https://data.nodc.noaa.gov/cgi-bin/iso?id=gov.noaa.nodc:0187104).

TABLES

Table 1. Summary of water column hydrographic parameters by region.

	Depth (m)		Temperature (°C)		Salinity		Dissolved Oxygen (mg L^{-1})		pH	
	2017	**2018**	**2017**	**2018**	**2017**	**2018**	**2017**	**2018**	**2017**	**2018**
GB										
Mean		0.82		27.51		26.06		6.42		7.90
Std. Dev.		0.22		0.63		2.61		0.96		0.15
SAB										
Mean		0.86		27.45		23.95		7.85		8.29
Std. Dev.		0.23		0.66		3.51		1.64		0.23
CB										
Mean	0.66	0.80	30.95	29.95	37.85	27.15	5.54	6.58	8.36	8.14
Std. Dev.	0.24	0.26	2.88	1.50	4.90	7.51	2.53	2.03	0.31	0.28
ULM										
Mean	1.04	1.11	29.25	26.95	41.52	33.74	5.89	6.33	8.32	8.07
Std. Dev.	0.52	0.47	3.92	3.58	5.54	1.47	1.48	1.31	0.24	0.20
LLM										
Mean	0.89	0.85	22.53	17.71	38.80	30.30	7.74	7.60	8.13	8.20
Std. Dev.	0.37	0.34	3.24	3.80	4.42	2.35	1.71	2.03	0.19	0.21

Table 2. Summary of water transparency property indicators by region.

	K_d (m^{-1})		Secchi (m)		Chlorophyll *a* (µg L^{-1})		Total Suspended Solids (mg L^{-1})	
	2017	**2018**	**2017**	**2018**	**2017**	**2018**	**2017**	**2018**
GB								
Mean		2.19		0.59		8.6		
Std. Dev.		0.95		0.17		3.2		
SAB								
Mean		2.11		0.66		7.2		23.5
Std. Dev.		1.40		0.20		2.9		19.9
CB								
Mean	1.04	1.32	0.63	0.72	5.0	4.3	11.7	7.8
Std. Dev.	0.36	0.69	0.21	0.25	3.5	3.3	7.4	6.1
ULM								
Mean	1.16	1.45	1.00	0.96	3.8	4.8	15.9	11.5
Std. Dev.	0.59	0.61	0.52	0.42	3.3	2.4	13.1	14.6
LLM								
Mean	1.00	0.99	0.80	0.83	1.3	3.3	8.1	8.2
Std. Dev.	0.50	0.51	0.31	0.33	1.5	3.3	6.8	8.9

Table 3. Summary of plant areal coverage by species and region.

		H. wrightii (% cover)		*T. testudinum* (% cover)		*S. filiforme* (% cover)		*R. maritima* (% cover)		*H. engelmannii* (% cover)		Bare (% cover)	
		2017	**2018**	**2017**	**2018**	**2017**	**2018**	**2017**	**2018**	**2017**	**2018**	**2017**	**2018**
GB													
	Mean		51.8		0		0		5.8		2.5		39.9
	Std. Dev.		33.7		0		0		9.8		6.9		37.1
SAB													
	Mean		50.8		0		0		5.2		1.0		41.3
	Std. Dev.		40.2		0		0		13.8		3.6		38.3
CB													
	Mean	33.7	37.6	25.1	24.2	5.9	8.1	1.0	0.8	0.3	1.0	33.9	28.3
	Std. Dev.	39.0	41.4	36.8	35.3	16.6	19.7	4.1	4.6	1.6	5.0	32.7	30.6
ULM													
	Mean	60.1	56.0	0	0	6.2	9.2	0	0	0.2	0.5	33.5	34.2
	Std. Dev.	36.6	35.8	0	0	16.2	20.6	0	0	1.4	2.8	35.3	34.8
LLM													
	Mean	34.2	31.6	24.1	23.8	2.2	2.4	0	0	1.4	0.5	38.0	41.6
	Std. Dev.	38.1	34.9	32.9	32.3	9.8	9.5	0	0.1	7.3	2.6	34.5	31.8

Table 4. Summary of plant canopy height by species and region.

		H. wrightii (cm)		*T. testudinum* (cm)		*S. filiforme* (cm)		*R. maritima* (cm)		*H. engelmannii* (cm)	
		2017	**2018**	**2017**	**2018**	**2017**	**2018**	**2017**	**2018**	**2017**	**2018**
GB											
	Mean		16.4		0		0		14.1		6.5
	Std. Dev.		6.4		0		0		6.1		1.7
SAB											
	Mean		22.7		0		0		16.9		6.6
	Std. Dev.		5.9		0		0		5.2		2.0
CB											
	Mean	18.0	17.7	34.3	30.4	23.9	26.2	13.2	12.0	5.6	5.3
	Std. Dev.	4.5	5.6	9.1	8.1	7.8	8.1	5.9	5.4	2.0	2.1
ULM											
	Mean	20.8	20.4	0	0	22.8	26.8	0	5.2	7.2	6.6
	Std. Dev.	7.0	7.6	0	0	6.8	6.9	0	0	1.4	2.2
LLM											
	Mean	15.6	13.5	18.5	19.2	18.5	24.9	0	11.9	5.6	5.1
	Std. Dev.	6.0	5.9	5.4	6.9	6.7	7.3	0	3.3	1.7	1.5

Table 5. Summary of plant tissue condition by species and region in 2017 and 2018.

		H. wrightii						*T. testudinum*					
		C:N		δ13C (‰)		δ15N (‰)		C:N		δ13C (‰)		δ15N (‰)	
		2017	2018	2017	2018	2017	2018	2017	2018	2017	2018	2017	2018
GB													
	Mean		17.7		-12.9		4.0						
	Std. Dev.		1.5		0.9		1.7						
SAB													
	Mean		18.3		-12.7		0.6						
	Std. Dev.		2.6		1.5		2.3						
CB													
	Mean	20.0	18.2	-11.9	-12.1	1.3	1.4	15.3	15.4	-10.2	-10.2	2.9	3.0
	Std. Dev.	2.3	2.5	1.4	3.3	2.6	2.2	1.9	1.7	1.1	0.7	1.4	1.6
ULM													
	Mean	20.7	17.2	-12.1	-14.4	2.5	2.9						
	Std. Dev.	2.7	2.1	1.5	1.2	1.3	1.7						
LLM													
	Mean	18.0	19.4	-9.9	-10.9	3.2	3.4	16.5	18.0	-9.5	-9.9	2.2	2.3
	Std. Dev.	1.8	2.7	1.4	1.8	2.4	2.4	2.5	2.6	1.0	1.8	1.7	1.7

FIGURES

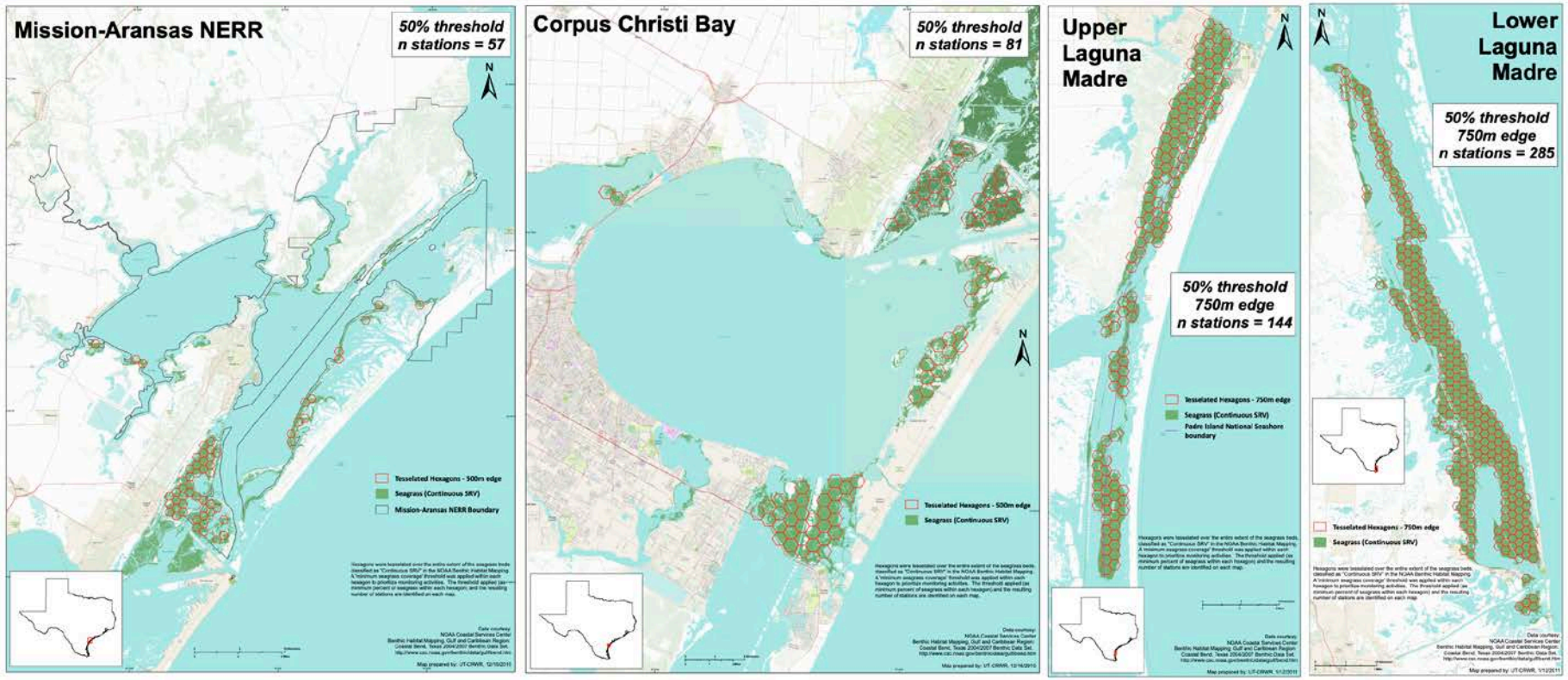

Figure 1. Tessellated boundaries of submerged vegetation delineated during the 2004/2007 NOAA Benthic Habitat Assessment. Seagrass sampling stations in each bay from left to right: Mission-Aransas National Estuarine Research Reserve, Corpus Christi Bay, Upper Laguna Madre, and Lower Laguna Madre. Mission-Aransas National Estuarine Research Reserve and Corpus Christi Bay are reported as the Coastal Bend.

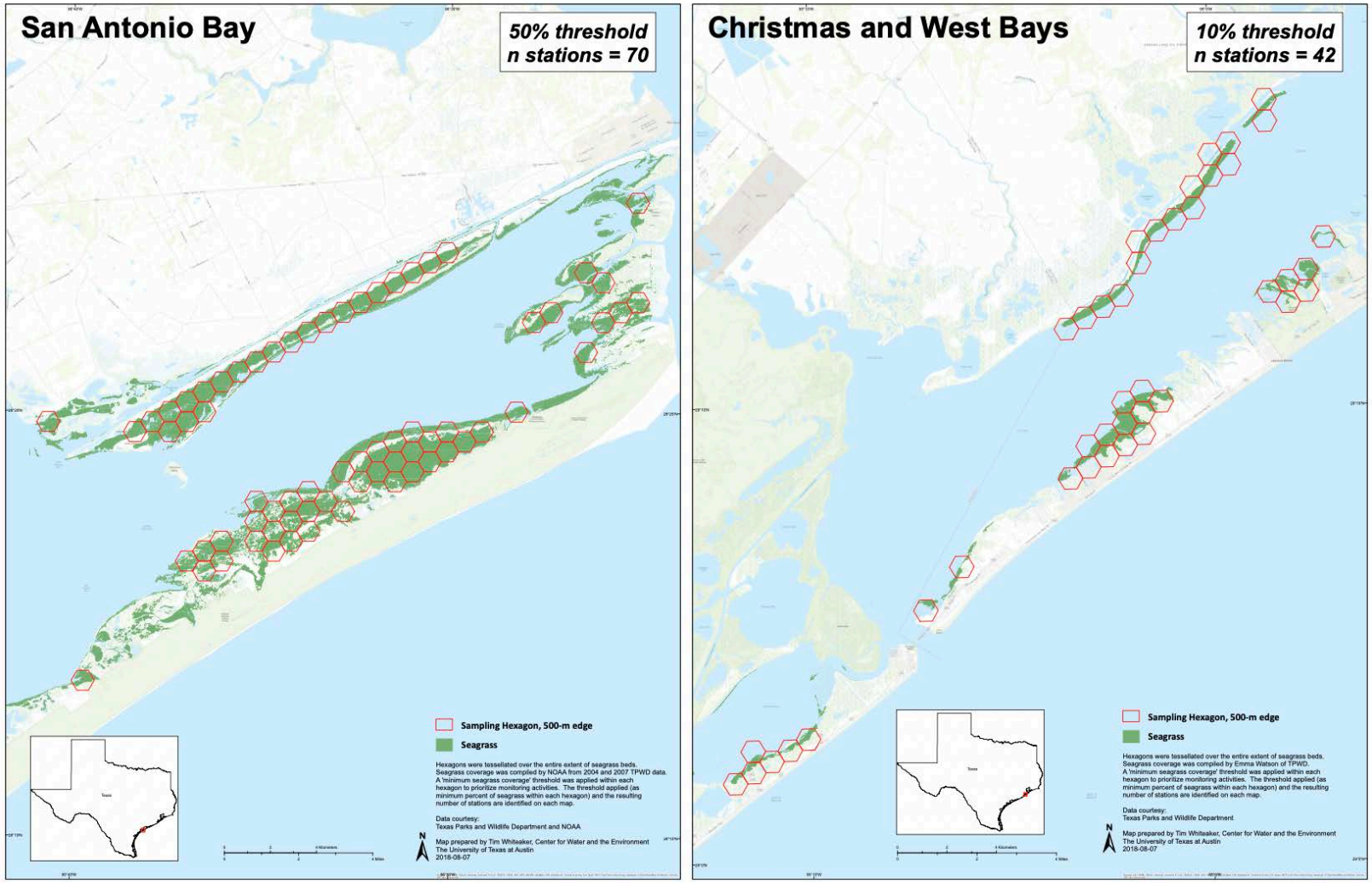

Figure 2. Tessellated boundaries of submerged vegetation delineated during the 2004/2007 NOAA Benthic Habitat Assessment. Seagrass sampling stations in each bay from left to right: San Antonio Bay, and Christmas and West Bays (reported as Galveston Bay).

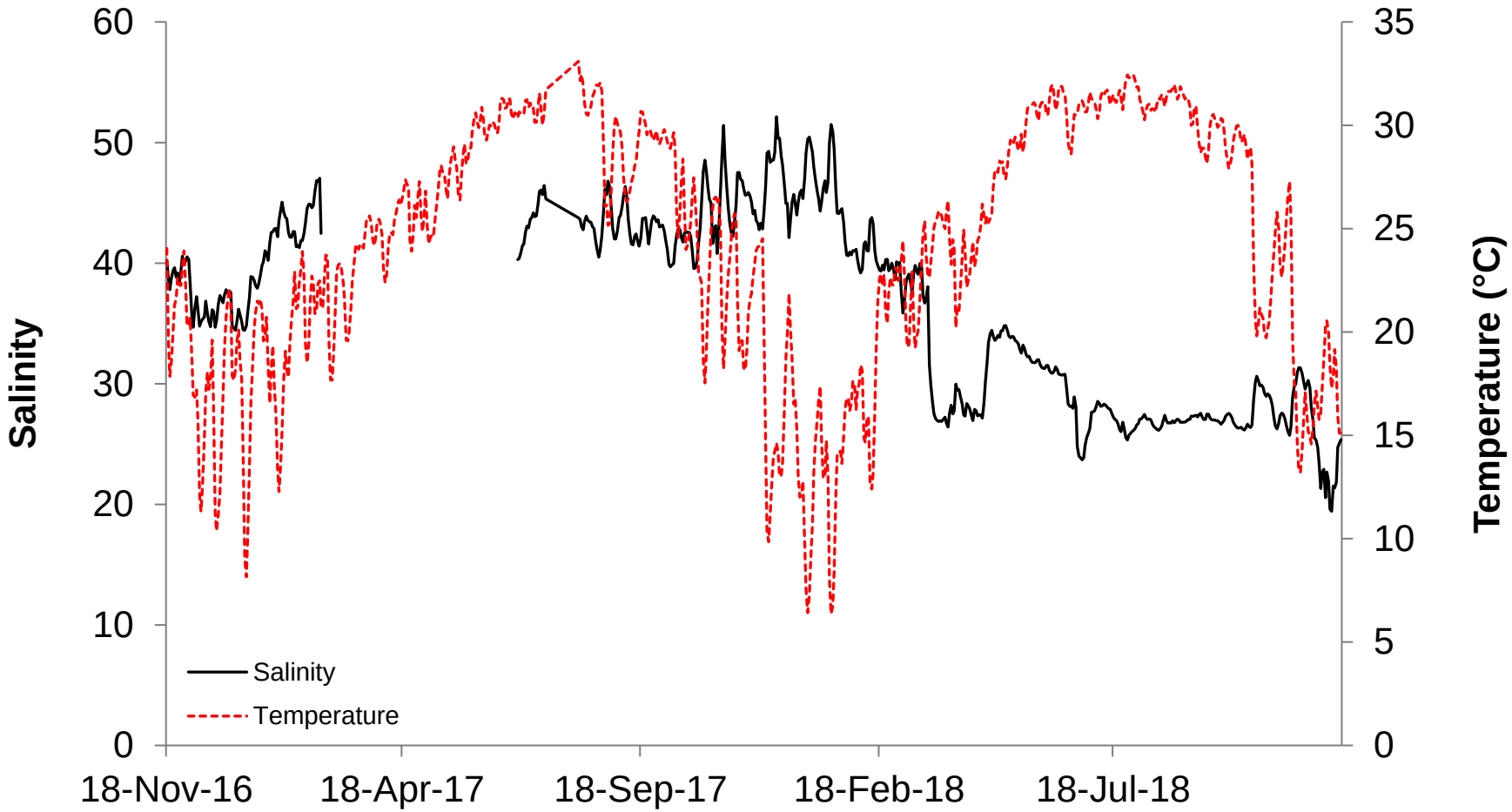

Figure 3. Mean daily salinity measurements from November 2016 to December 2018 for Upper Laguna Madre, TX near Padre Island National Seashore.

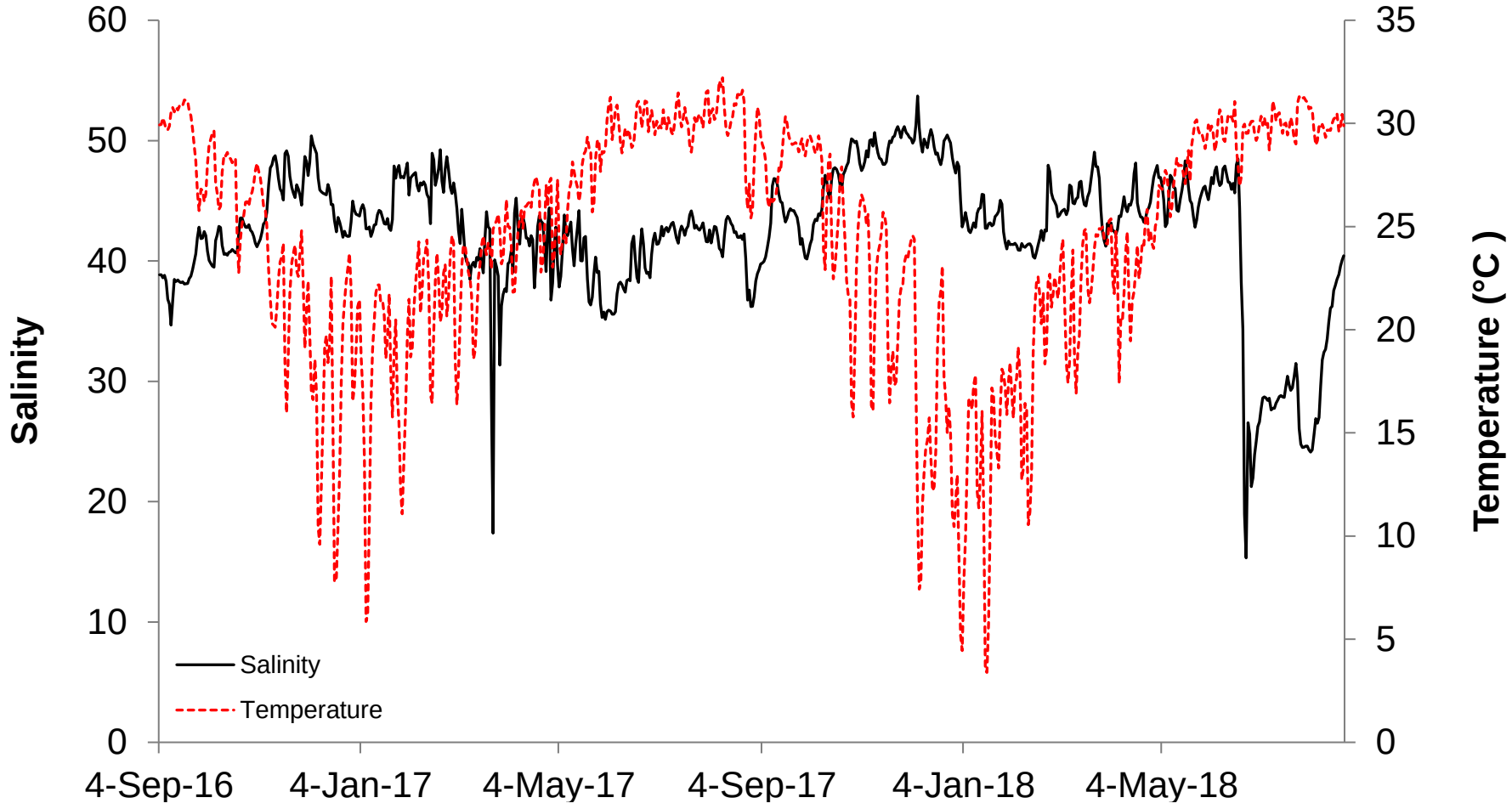

Figure 4. Mean daily salinity measurements from September 2016 to August 2018 for southern Upper Laguna Madre, TX near Nine Mile Hole.

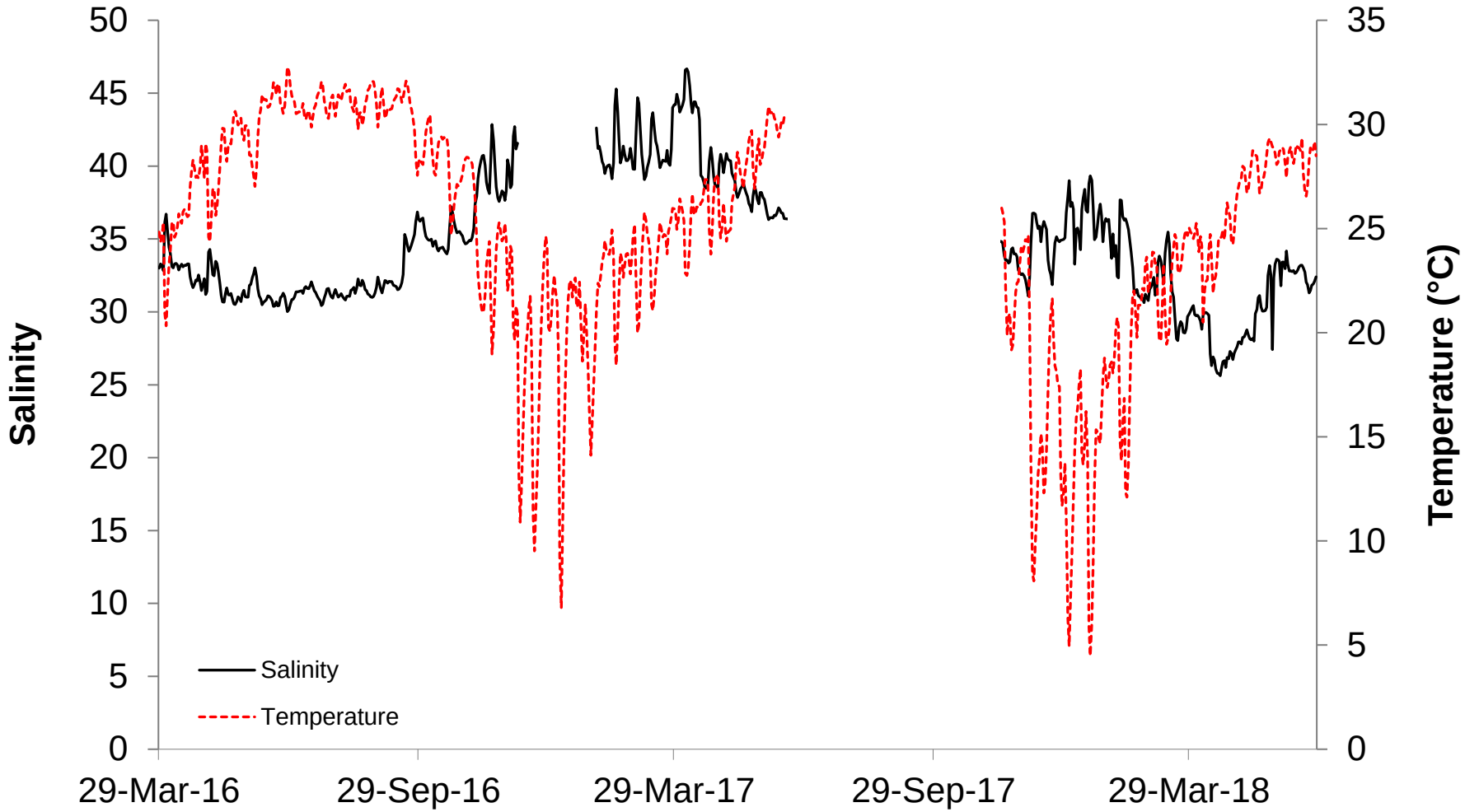

Figure 5. Mean daily salinity measurements from March 2016 to June 2018 for southern Lower Laguna Madre, TX near South Padre Island.

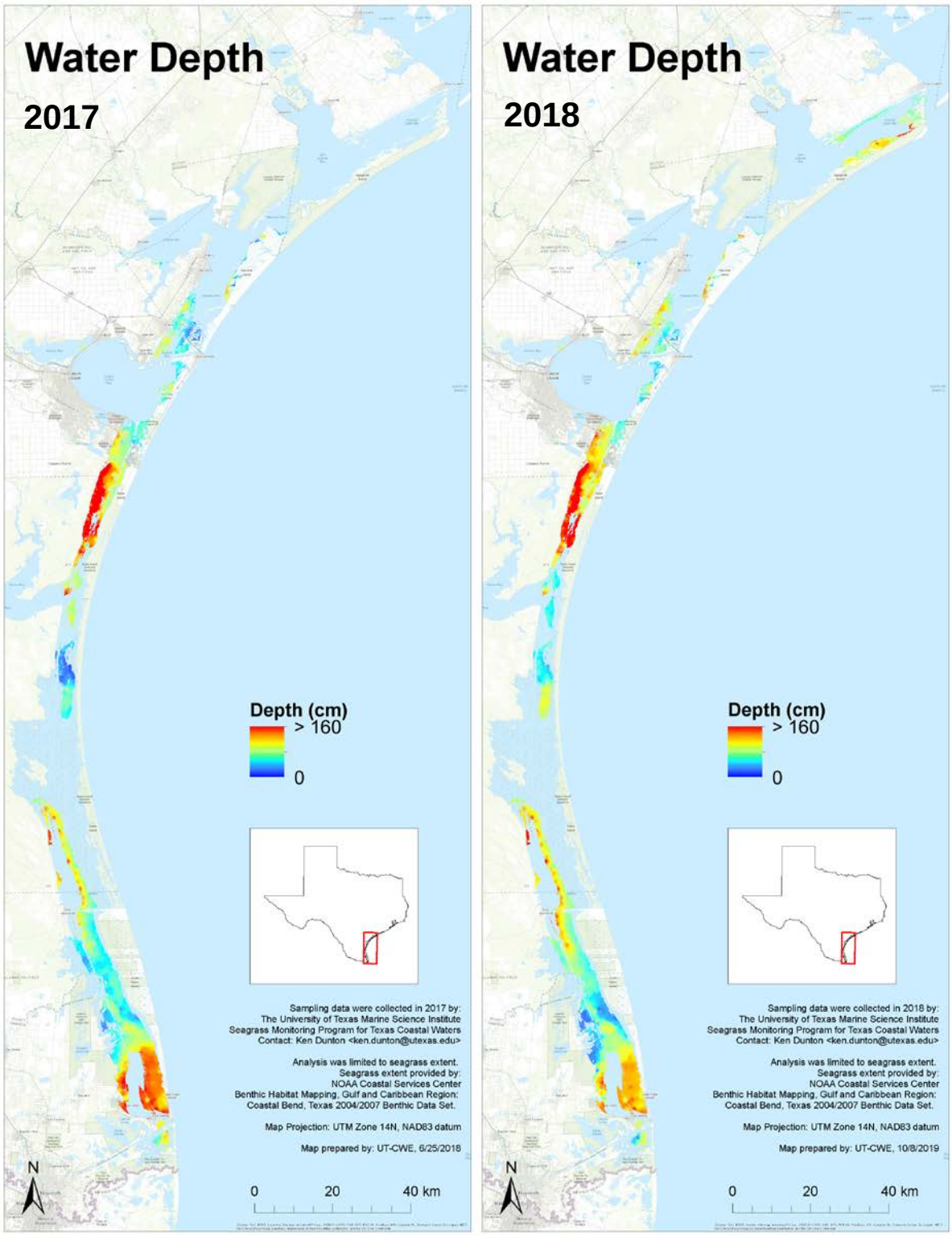

Figure 6. Spatial representations of water depth for 2017 (left) and 2018 (right). The spatial data interpolation is limited to the boundaries of seagrass habitat delineated during the 2004/2007 NOAA Benthic Habitat Assessment.

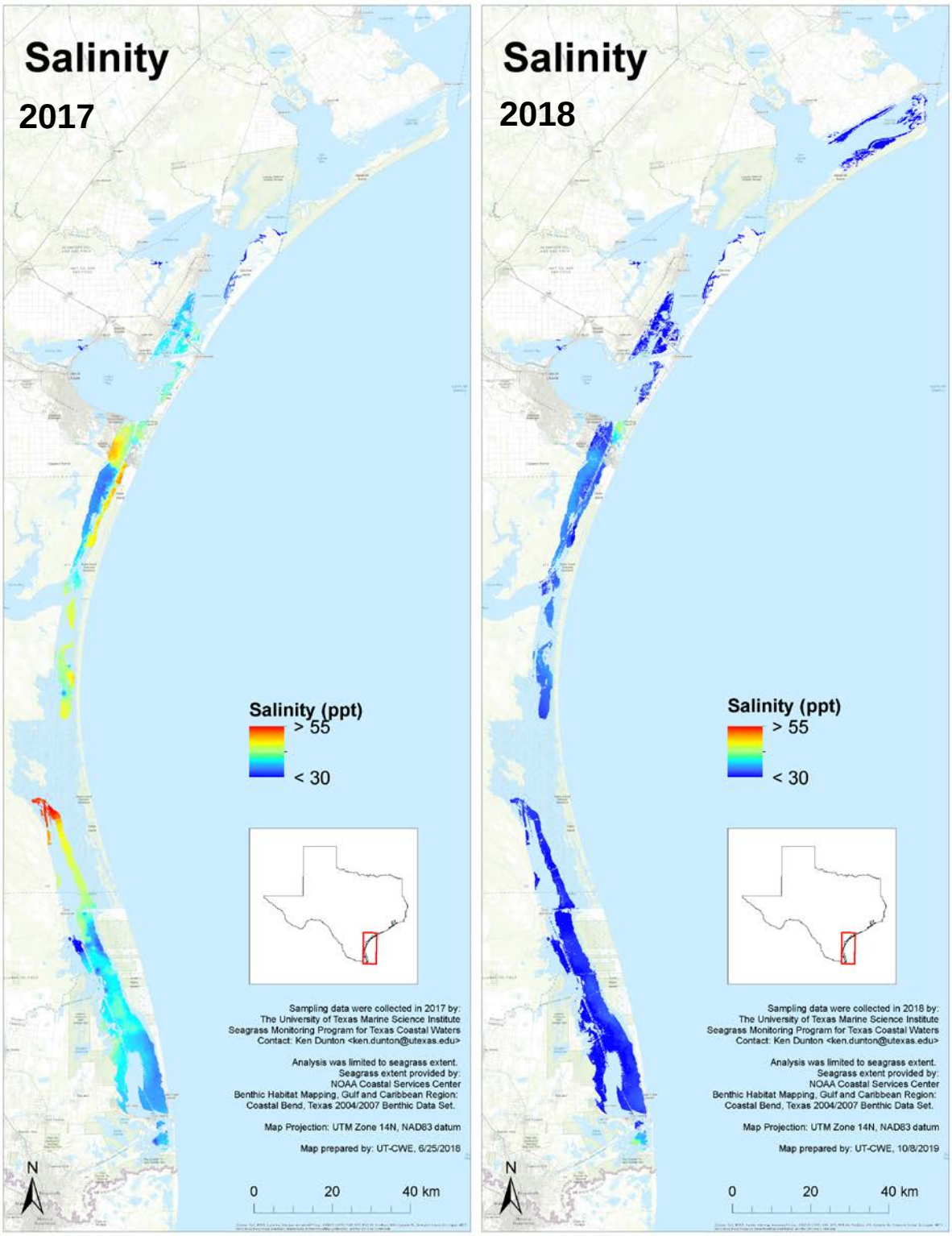

Figure 7. Spatial representations of salinity for 2017 (left) and 2018 (right). The spatial data interpolation is limited to the boundaries of seagrass habitat delineated during the 2004/2007 NOAA Benthic Habitat Assessment.

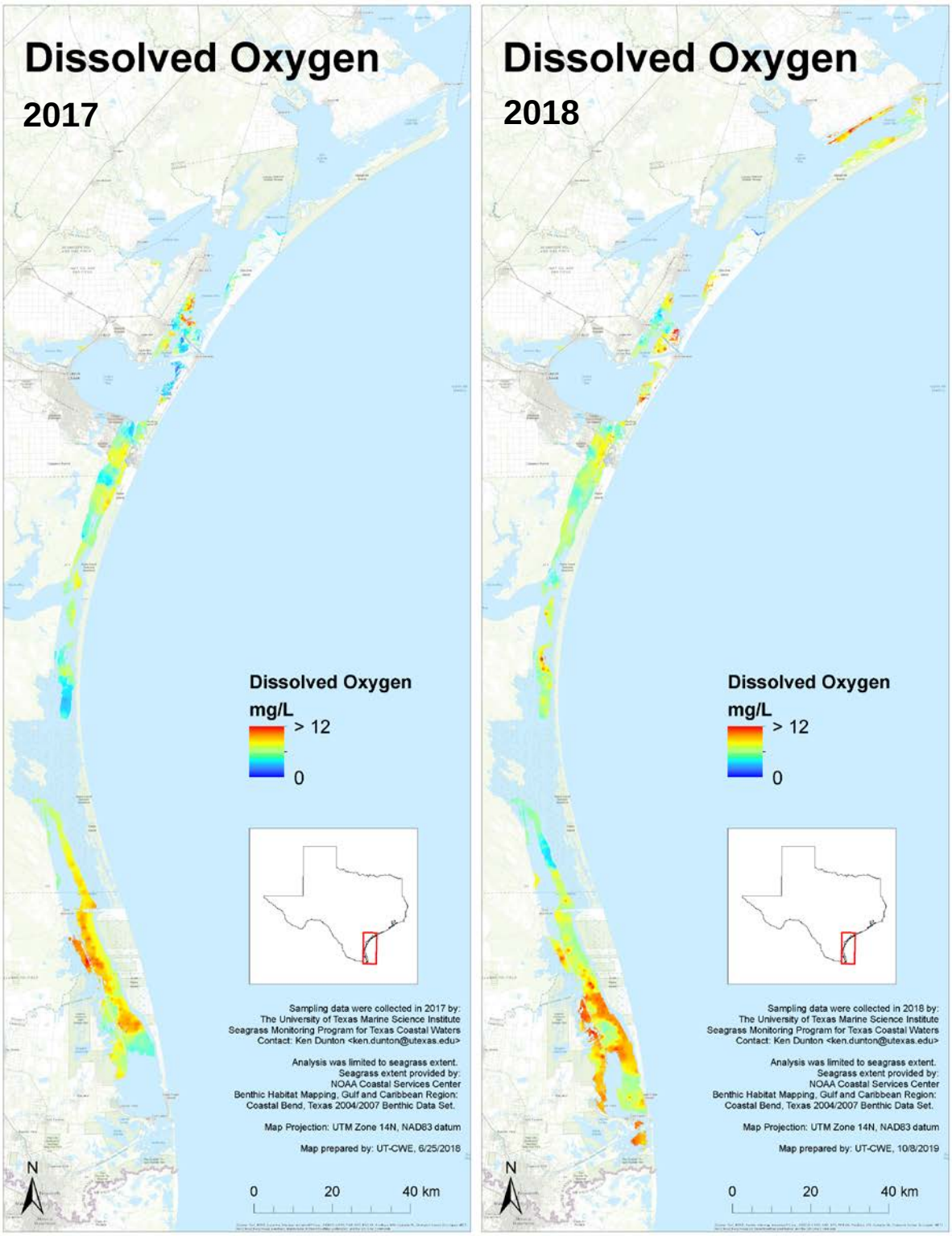

Figure 8. Spatial representations of dissolved oxygen for 2017 (left) and 2018 (right). The spatial data interpolation is limited to the boundaries of seagrass habitat delineated during the 2004/2007 NOAA Benthic Habitat Assessment.

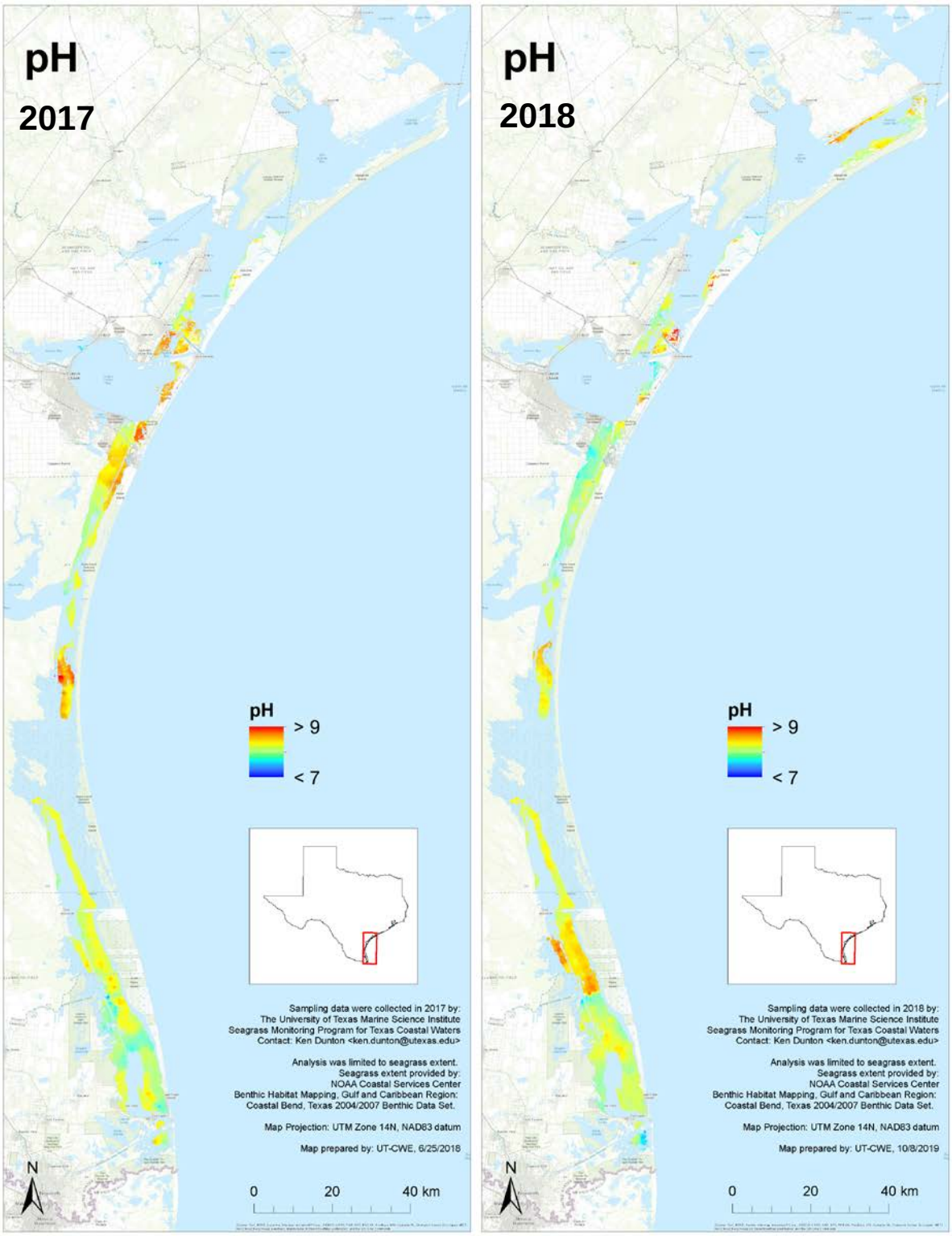

Figure 9. Spatial representations of pH for 2017 (left) and 2018 (right). The spatial data interpolation is limited to the boundaries of seagrass habitat delineated during the 2004/2007 NOAA Benthic Habitat Assessment.

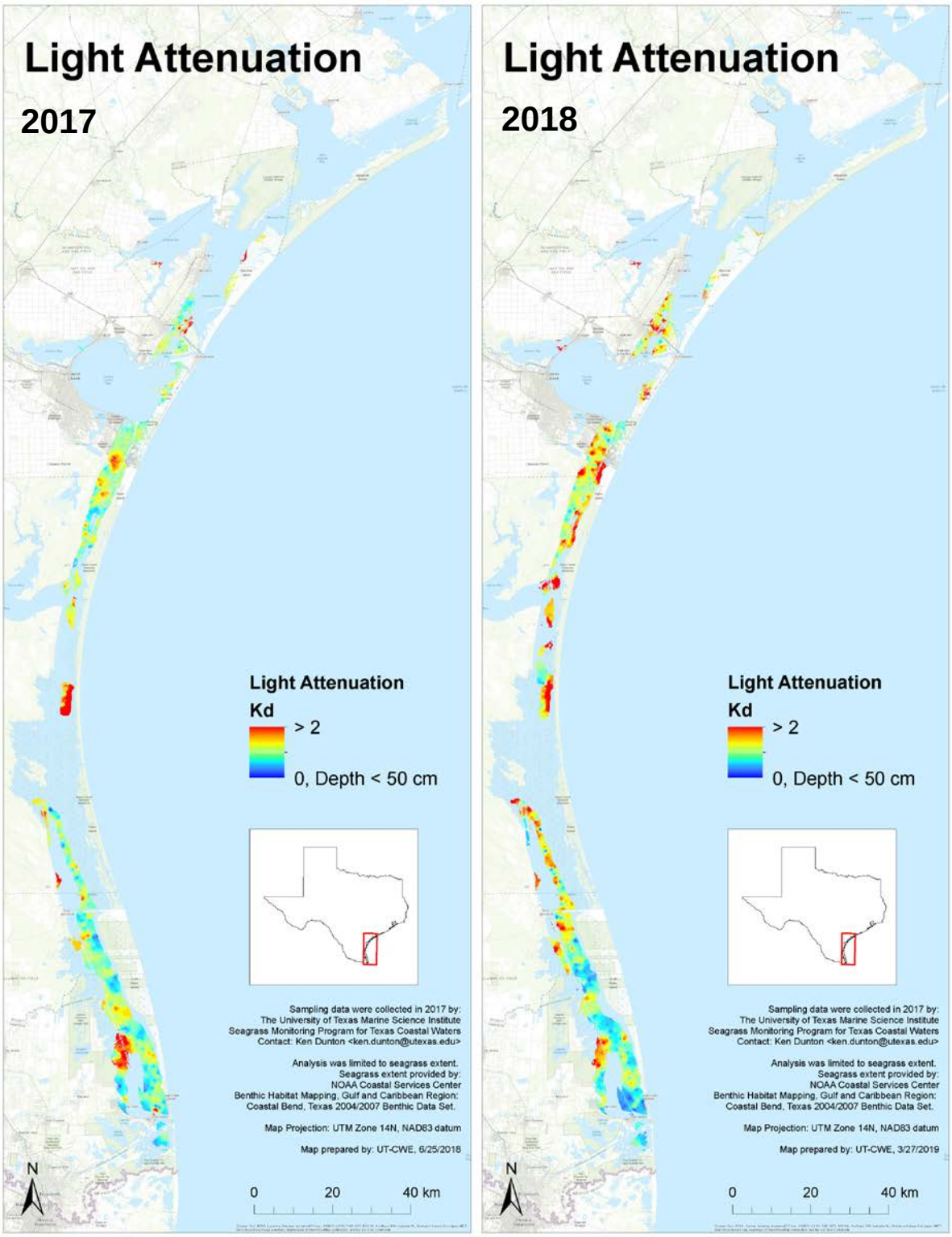

Figure 10. Spatial representations of light attenuation for 2017 (left) and 2018 (right). The spatial data interpolation is limited to the boundaries of seagrass habitat delineated during the 2004/2007 NOAA Benthic Habitat Assessment.

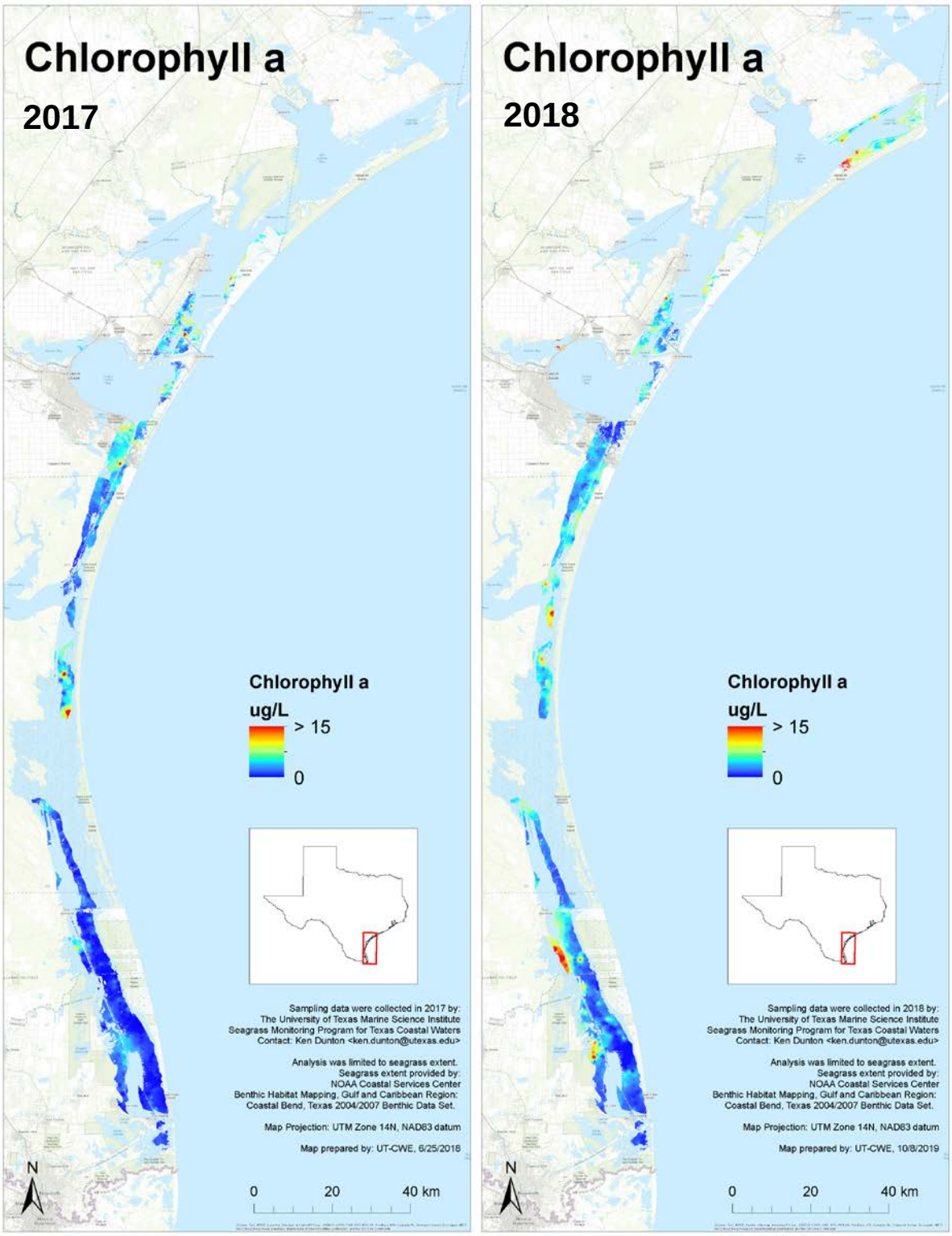

Figure 11. Spatial representations of chlorophyll *a* for 2017 (left) and 2018 (right). The spatial data interpolation is limited to the boundaries of seagrass habitat delineated during the 2004/2007 NOAA Benthic Habitat Assessment.

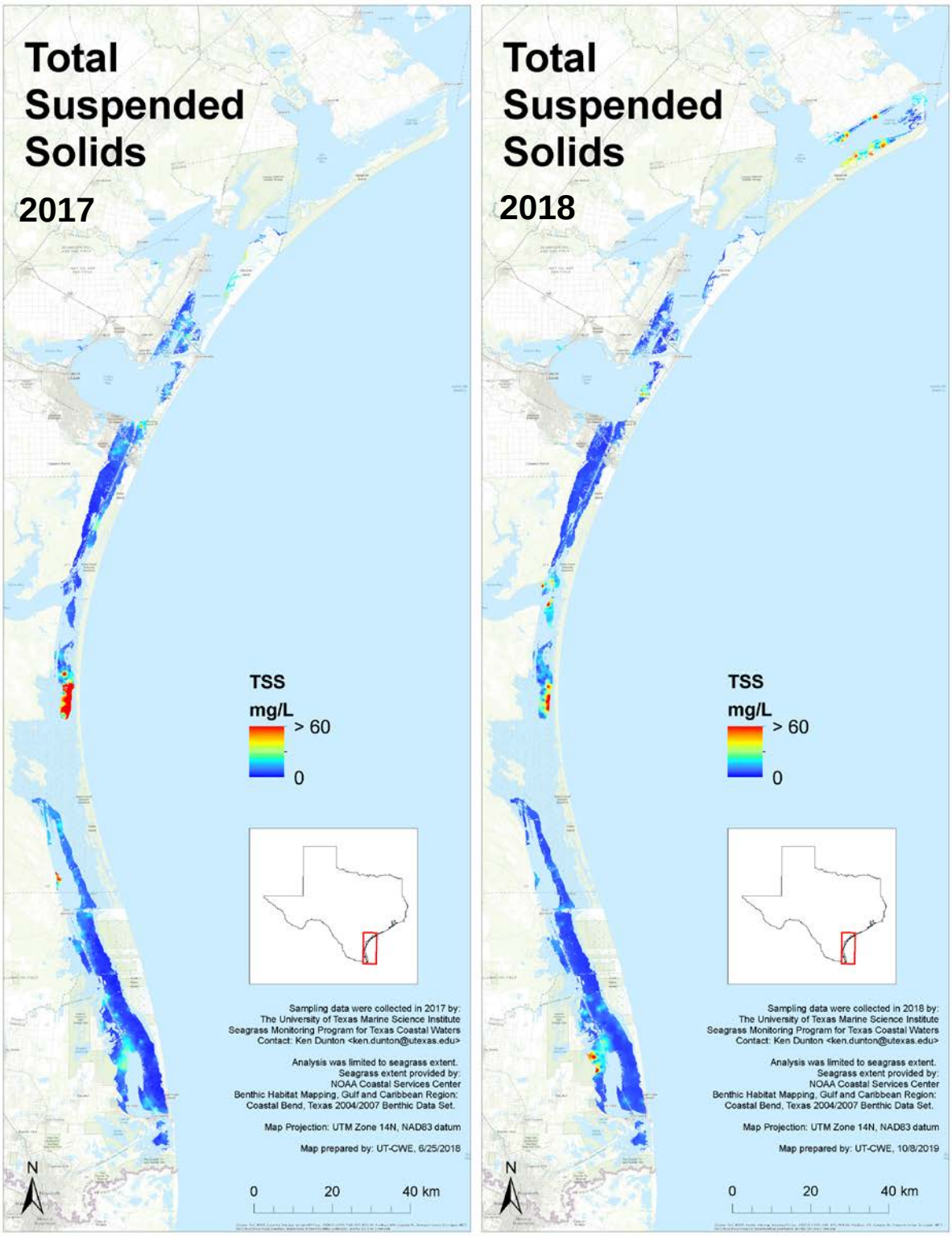

Figure 12. Spatial representations of total suspended solids for 2017 (left) and 2018 (right). The spatial data interpolation is limited to the boundaries of seagrass habitat delineated during the 2004/2007 NOAA Benthic Habitat Assessment.

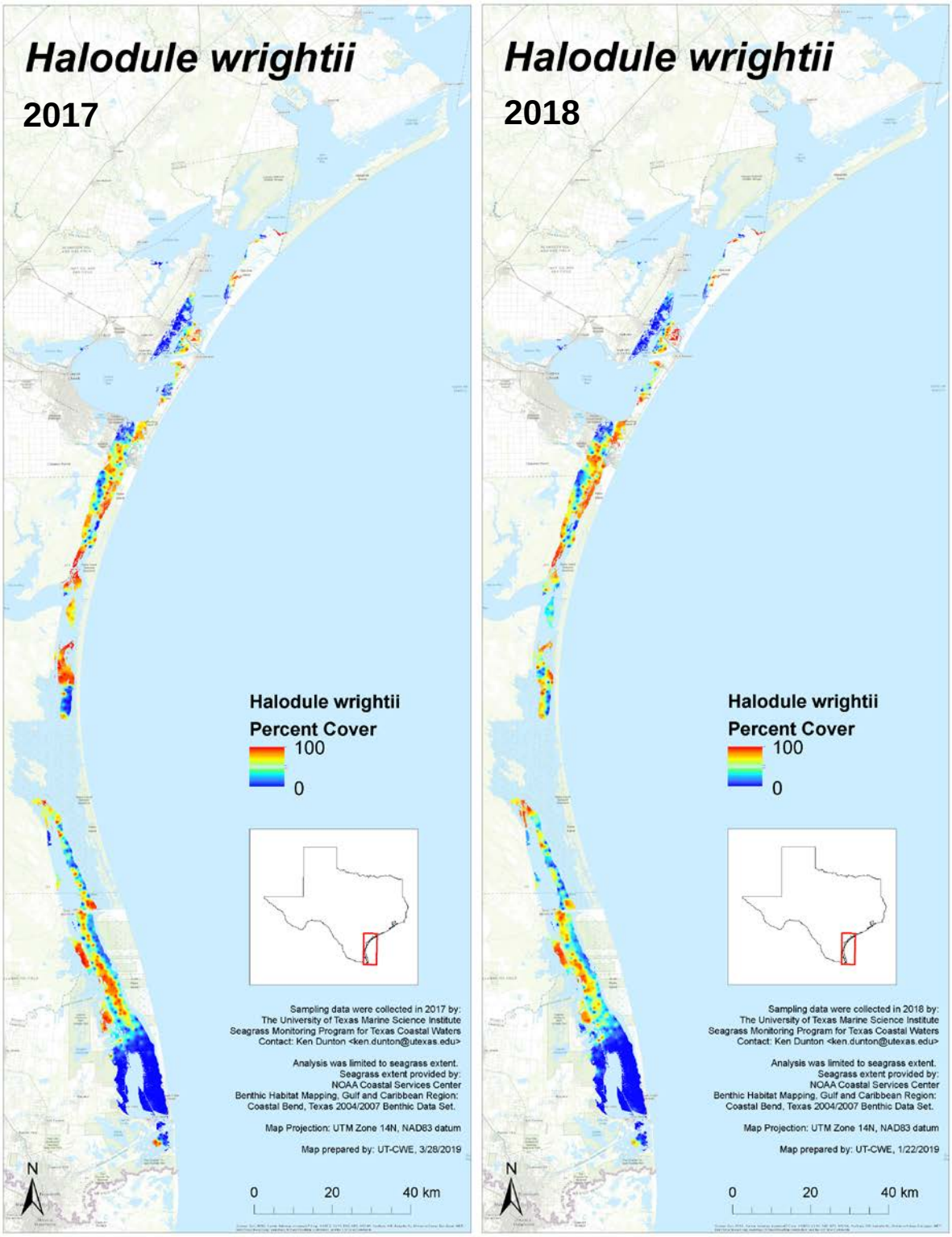

Figure 13. Spatial representations of percent cover of *Halodule wrightii* for 2017 (left) and 2018 (right). The spatial data interpolation is limited to the boundaries of seagrass habitat delineated during the 2004/2007 NOAA Benthic Habitat Assessment.

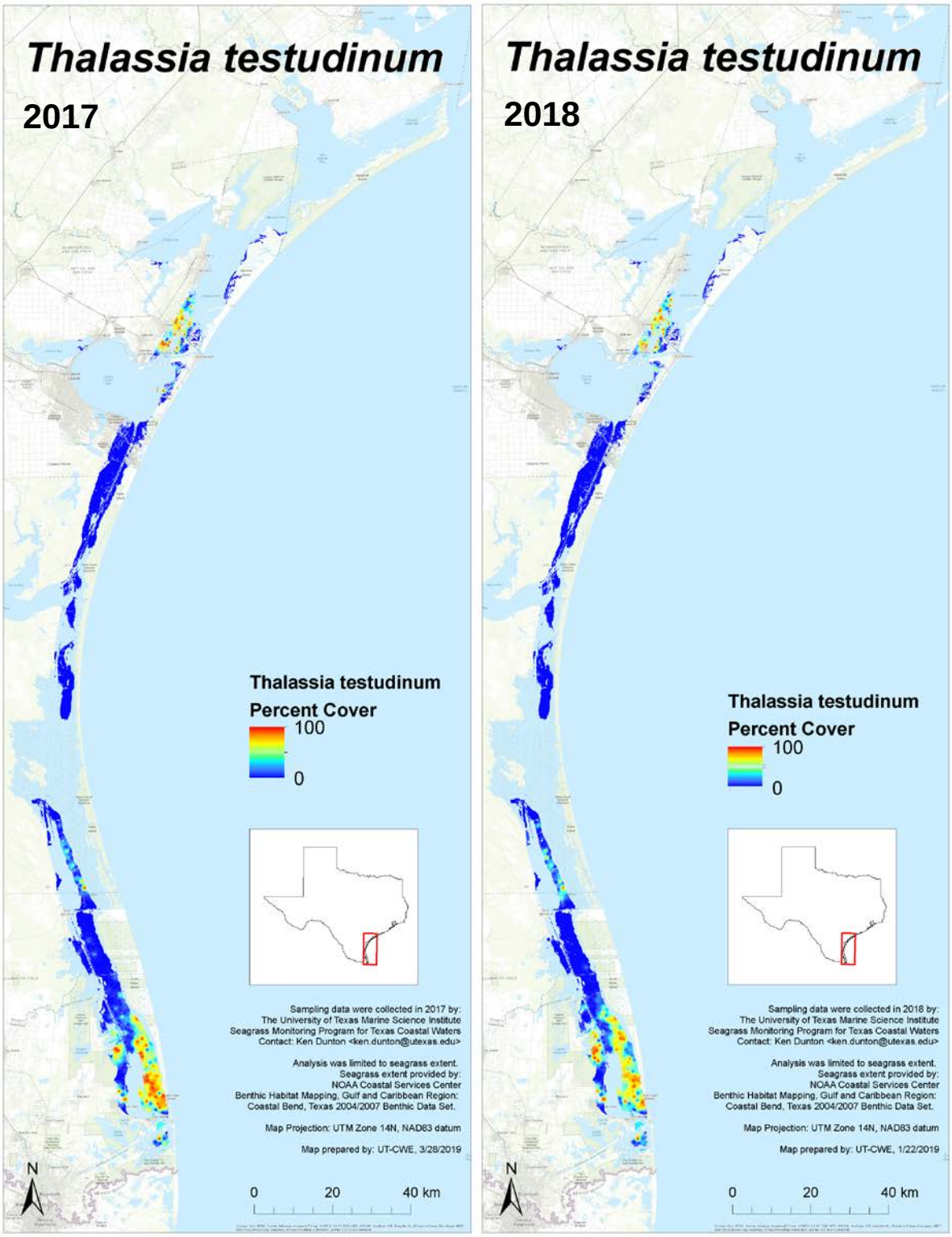

Figure 14. Spatial representations of percent cover of *Thalassia testudinum* for 2017 (left) and 2018 (right). The spatial data interpolation is limited to the boundaries of seagrass habitat delineated during the 2004/2007 NOAA Benthic Habitat Assessment.

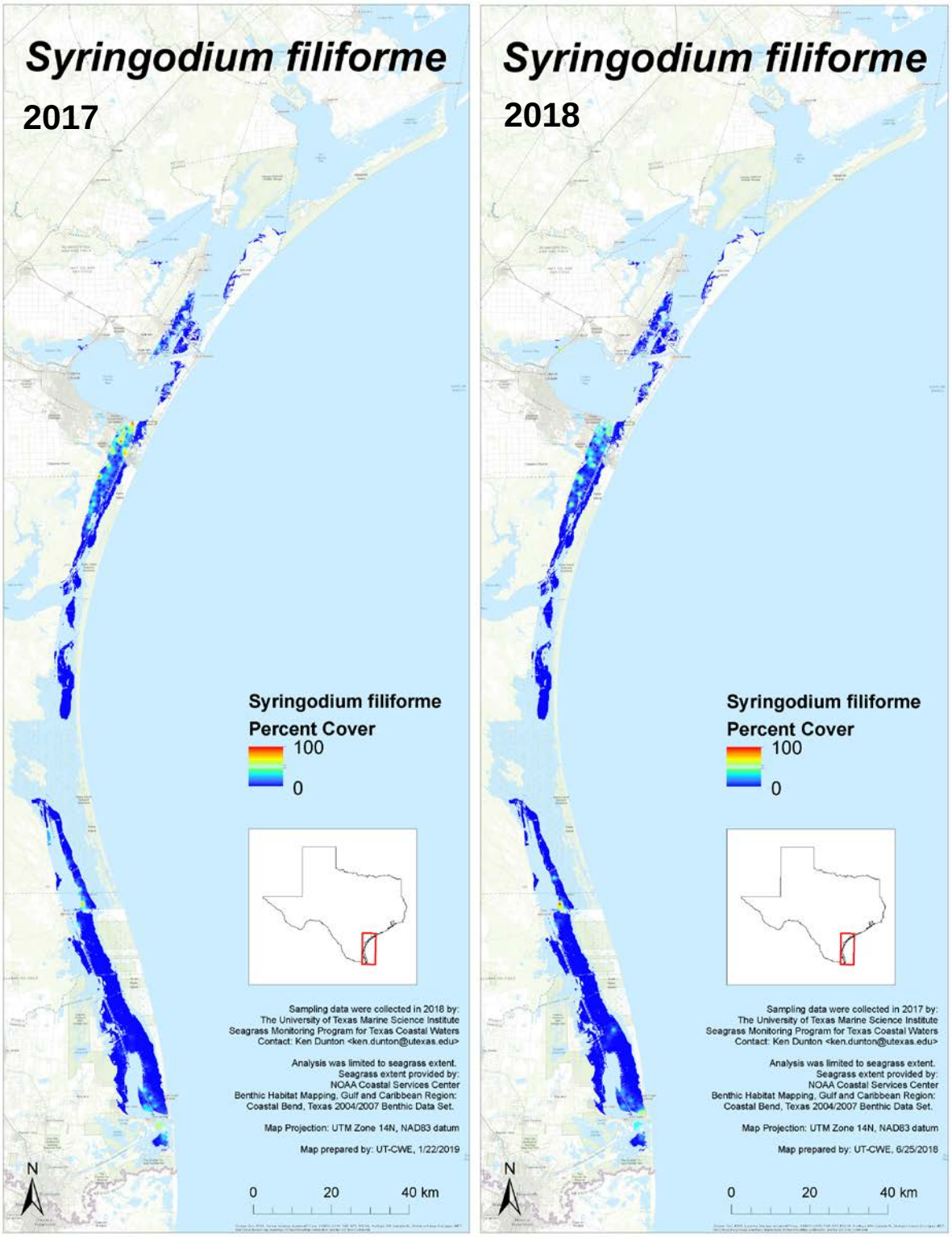

Figure 15. Spatial representations of percent cover of *Syringodium filiforme* for 2017 (left) and 2018 (right). The spatial data interpolation is limited to the boundaries of seagrass habitat delineated during the 2004/2007 NOAA Benthic Habitat Assessment.

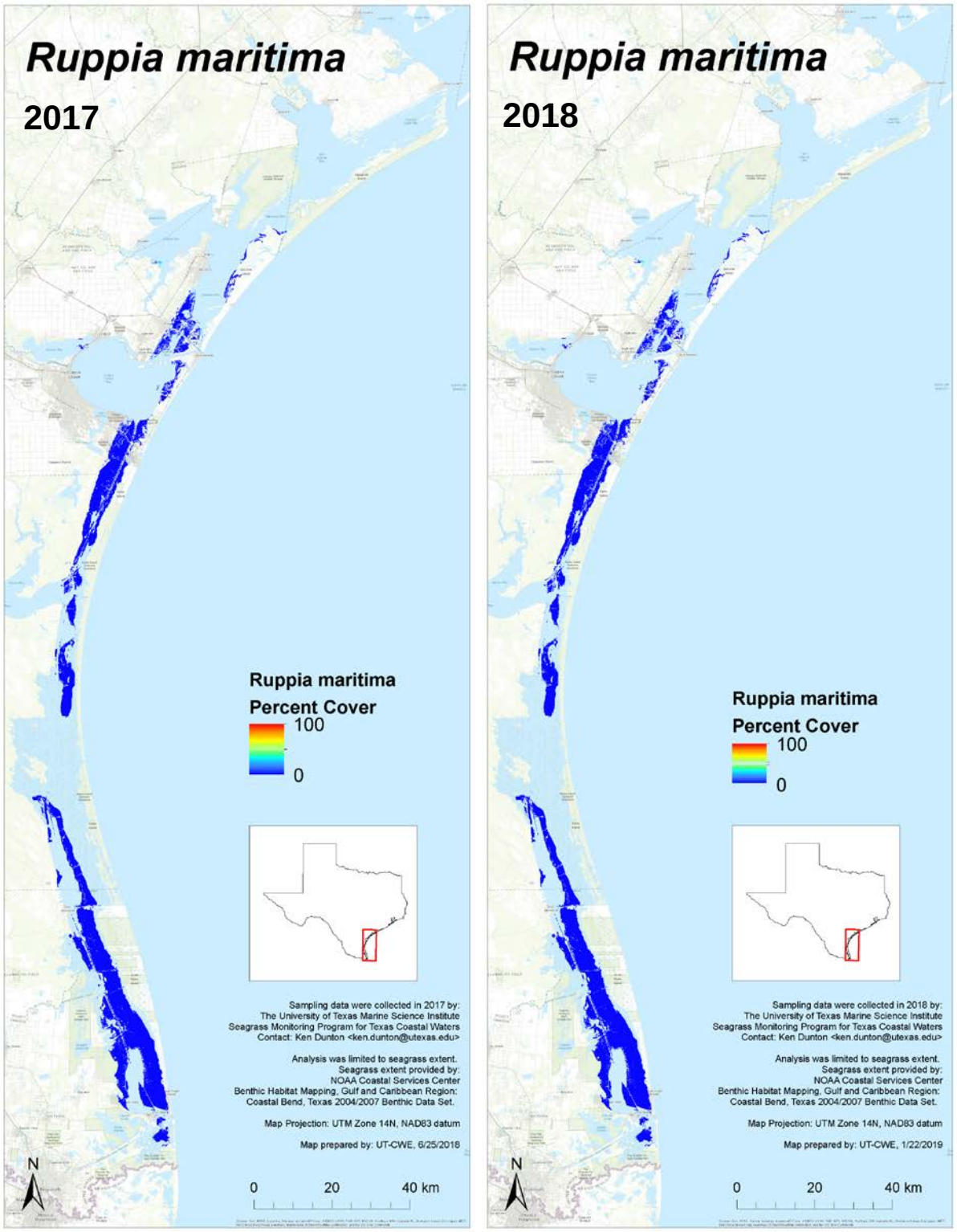

Figure 16. Spatial representations of percent cover of *Ruppia maritima* for 2017 (left) and 2018 (right). The spatial data interpolation is limited to the boundaries of seagrass habitat delineated during the 2004/2007 NOAA Benthic Habitat Assessment.

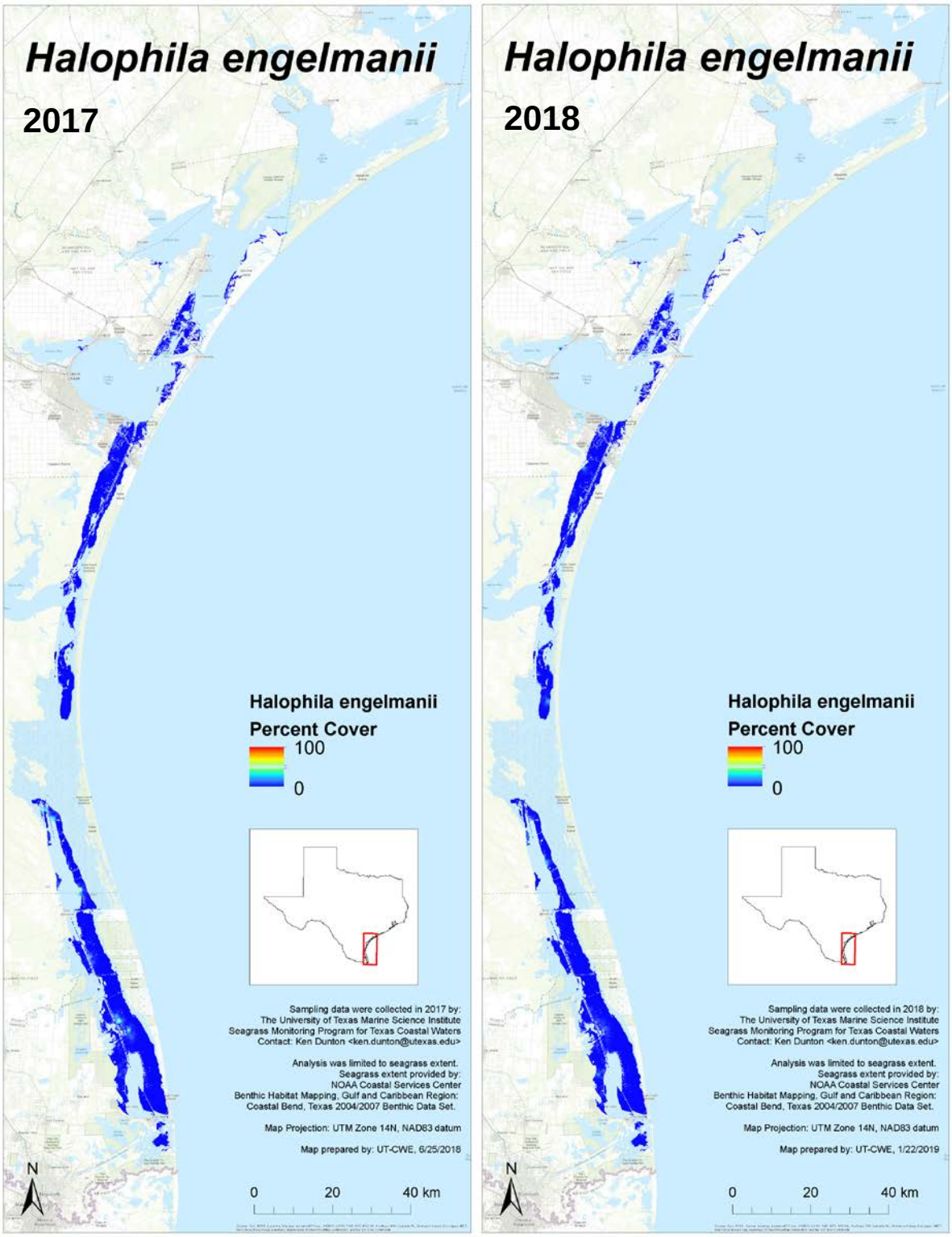

Figure 17. Spatial representations of percent cover of *Halophila engelmannii* for 2017 (left) and 2018 (right). The spatial data interpolation is limited to the boundaries of seagrass habitat delineated during the 2004/2007 NOAA Benthic Habitat Assessment.

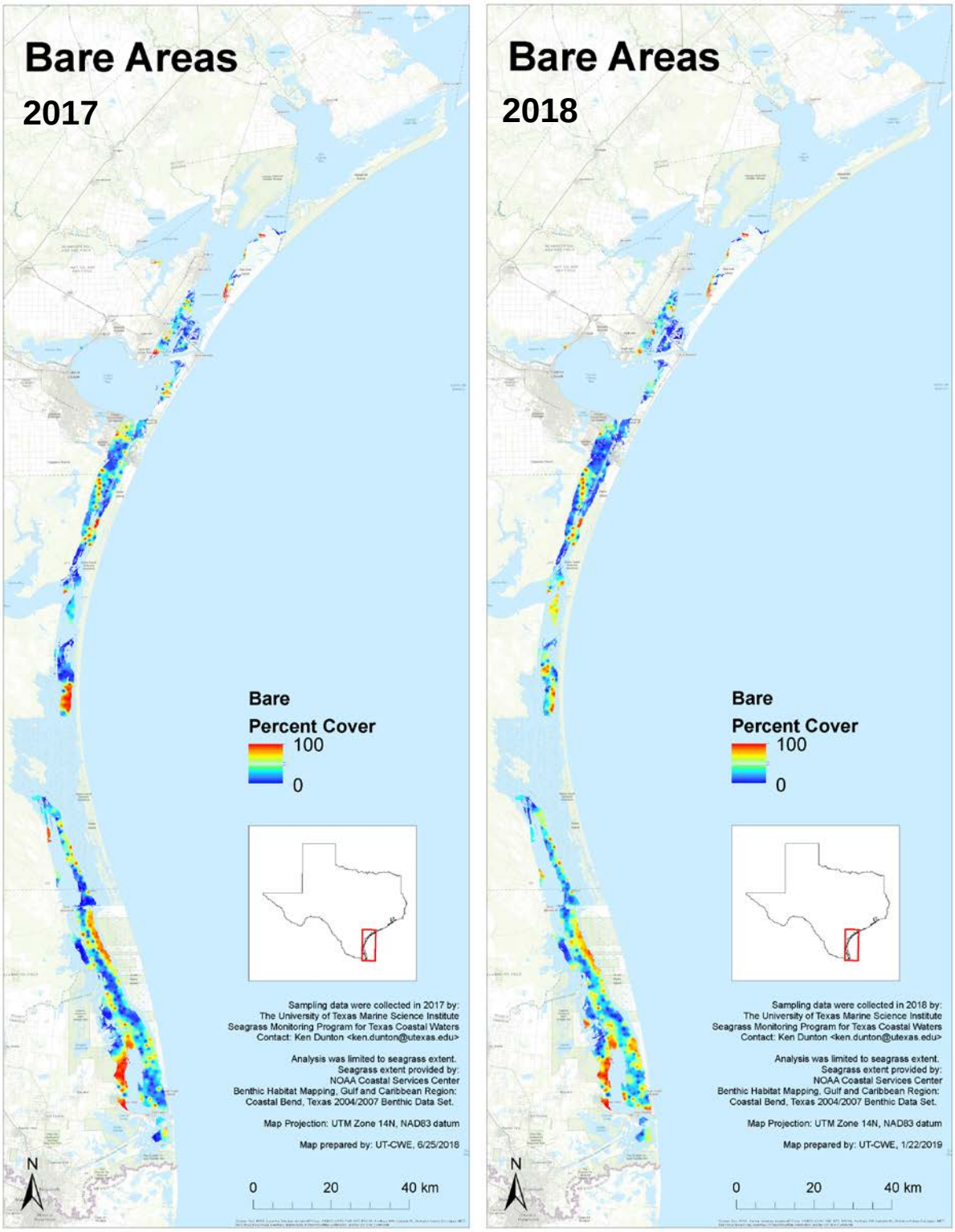

Figure 18. Spatial representations of percent cover of bare areas for 2017 (left) and 2018 (right). The spatial data interpolation is limited to the boundaries of seagrass habitat delineated during the 2004/2007 NOAA Benthic Habitat Assessment.

REFERENCES

Congdon, V.M., C. Bonsell, M.R. Cuddy, and K.H. Dunton. 2019. In the wake of a major hurricane: Differential effects on early vs. late successional seagrass species. *Limnology and Oceanography Letters* 4:155-163.

Dennison, W.C., R.J. Orth, K.A. Moore, J.C. Stevenson, V. Carter, S. Kollar, P.W. Bergstrom, and R.A. Batiuk. 1993. Assessing Water Quality with Submersed Aquatic Vegetation. *BioScience* 43:86-94.

Dunton, K.H., J.L. Goodall, S.V. Schonberg, J.M. Grebmeier, and D.R. Maidment. 2005. Multi-decadal synthesis of benthic-pelagic coupling in the western arctic: role of cross-shelf advective processes. *Deep-Sea Research II* 52:3462-3477.

Dunton, K H., W. Pulich, Jr. and T. Mutchler. 2011. A seagrass monitoring program for Texas coastal waters. http://www.texasseagrass.org/. 39 pp.

Fourqurean, J.W., M.J. Durako, M.O. Hall, and L.N. Hefty. 2002. Seagrass distribution in south Florida: a multi-agency coordinated monitoring program. *In: Linkages between ecosystems in the south Florida hydroscape: the river of grass continues*. Porter, J.W., and K.G. Porter (eds). CRC Press.

Fourqurean, J.W., J.N. Boyer, M.J. Durako, L.N. Hefty, and B.J. Peterson. 2003. Forecasting responses of seagrass distributions to changing water quality using monitoring data. *Ecological Applications* 13:474-489.

Fourqurean, J.W., C.M. Duarte, H. Kennedy, N. Marba, M. Holmer, M.A. Mateo, E.T. Apostolaki, G.A. Kendrick, D. Krause-Jensen, K.J. McGlathery, and O. Serrano. 2012. Seagrass ecosystems as a globally significant carbon stock. *Nature Geoscience* 5:505-509.

Kirkman, H. 1996. Baseline and Monitoring Methods for Seagrass Meadows. *Journal of Environmental Management* 47:191-201.

Koch, E.W. 2001. Beyond light: Physical, geological, and geochemical parameters as possible submersed aquatic vegetation habitat requirements. *Estuaries and Coasts* 24:1-17.

Livingston, R.J., S.E. McGlynn, and N. Xufeng. 1998. Factors Controlling Seagrass Growth in a Gulf Coastal System: Water and Sediment Quality and Light. *Aquatic Botany* 60: 135-159.

Mateo, M.A., J. Cebrián, K. Dunton, and T. Mutchler. 2006. Carbon Flux in Seagrass Ecosystems. In: *Seagrasses: Biology, Ecology and Conservation*. Larkum, A.W.D., et al (eds.), pp. 159-192, Springer.

Neckles, H. A., B. S. Kopp, B. J. Peterson, and P. S. Pooler. 2011. Integrating scales of seagrass monitoring to meet conservation needs. Estuaries and Coasts: In press.

Pulich, W.M., Jr. and T. Calnan. (eds.) 1999. Seagrass Conservation Plan for Texas. Resource Protection Division. Austin, Texas: Texas Parks and Wildlife Department. 67 p.

Pulich, W.M., Jr., B. Hardegree, A. Kopecky, S. Schwelling, C. P. Onuf, and K.H. Dunton. 2003. Texas Seagrass Monitoring Strategic Plan (TSMSP). Publ. Texas Parks and Wildlife Department, Resource Protection Division, Austin, Texas. 27 p.

Wilson, S.S., and K.H. Dunton. 2017. Hypersalinity During Regional Drought Drives Mass Mortality of the Seagrass *Syringodium filiforme* in a Subtropical Lagoon. *Estuaries and Coasts* 41:855-865.

APPENDIX: METHODS

A.1 Total Suspended Solids

Developed by: Kenneth Dunton and Kimberly Jackson
Adapted from: EPA METHOD #: 160.2
Approved by: TPWD (2010)

1.0 Scope and Application
This method is applicable to drinking, surface, and saline waters, domestic and industrial wastes. The practical range of the determination is 4 mg/L to 20,000 mg/L.

2.0 Summary of Method
A well-mixed sample is filtered through a glass fiber filter, and the residue retained on the filter is dried to constant weight at 103-105°C. The filtrate from this method may be used for Residue, Filterable. Residue, and Non-Filterable. These are defined as those solids which are retained by a glass fiber filter and dried to constant weight at 103-105°C.

3.0 Sample Handling and Preservation
Non-representative particulates such as leaves, sticks, fish, and lumps of fecal matter should be excluded from the sample if it is determined that their inclusion is not desired in the final result. Preservation of the sample is not practical; analysis should begin as soon as possible. Refrigeration or icing to 4°C, to minimize microbiological decomposition of solids, is recommended.

4.0 Interferences
Filtration apparatus, filter material, pre-washing, post-washing, and drying temperature are specified because these variables have been shown to affect the results. Samples high in Filterable Residue (dissolved solids), such as saline waters, brines and some wastes, may be subject to a positive interference. Care must be taken in selecting the filtering apparatus so that washing of the filter and any dissolved solids in the filter (7.5) minimizes this potential interference.

5.0 Procedure
1) Place the glass fiber filter (i.e., Glass fiber filter discs, without organic binder, such as Millipore AP-40, Reeves Angel 934-AH, Gelman type A/E, or equivalent Our lab uses 47 mm GF/F 0.7 micron retention on the membrane filter apparatus. NOTE: Because of the physical nature of glass fiber filters, the absolute pore size cannot be controlled or measured. Terms such as "pore size", collection efficiencies and effective retention are used to define this property in glass fiber filters.

2) Dry new filters at 60C in oven prior to use.

3) Weigh filter immediately before use. After weighing, handle the filter or crucible/filter with forceps or tongs only.

4) For a 47 mm diameter filter, filter 100 mL of sample. If weight of captured residue is less than 1.0 mg, the sample volume must be increased to provide at least 1.0 mg of residue. If other filter diameters are used, start with a sample volume equal to 7 mL/cm of filter area and collect at least a weight of residue proportional to the 1.0 mg stated above. Note: If filtering clear pristine water, start with 1L. If filtering turbid water start with 100 m.

NOTE: If during filtration of this initial volume the filtration rate drops rapidly, or if filtration time exceeds 5 to 10 minutes, the following scheme is recommended: Use an unweighed glass fiber filter of choice affixed in the filter assembly. Add a known volume of sample to the filter funnel and record the time elapsed after selected volumes have passed through the filter. Twenty- five mL increments for timing are suggested. Continue to record the time and volume increments until filtration rate drops rapidly. Add additional sample if the filter funnel volume is inadequate to reach a reduced rate. Plot the observed time versus volume filtered. Select the proper filtration volume as that just short of the time a significant change in filtration rate occurred.

5) Assemble the filtering apparatus and begin suction.

6) Shake the sample vigorously and quantitatively transfer the predetermined sample volume selected to the filter using a graduated cylinder. Pour into funnel.

7) Remove all traces of water by continuing to apply vacuum after sample has passed through.

8) With suction on, wash the graduated cylinder, filter, non-filterable residue and filter funnel wall with three portions of distilled water allowing complete drainage between washing. Remove all traces of water by continuing to apply vacuum after water has passed through.

NOTE: Total volume of distilled rinse water used should equal no less than 50mls following complete filtration of sample volume.

9) Carefully remove the filter from the filter support.
10) Dry at least one hour at 103-105°C. Overnight insures accurate filter weight.
11) Cool in a desiccator and weigh.
12) Repeat the drying cycle until a constant weight is obtained (weight loss is less than 0.5 mg).

6.0 Calculations
Calculate non-filterable residue as follows, where: A = weight of filter (or filter and crucible) + residue in mg B = weight of filter (or filter and crucible) in mg C = mL of sample filtered

1000*(A-B)*1000/C=TSS mg/L

A.2 Percent Surface Irradiance and Light Attenuation

Developed by: Kenneth Dunton and Kimberly Jackson
Last Revised: December 2009
Approved by: EPA (2002) and TPWD (2010)

Field Measurements

Measurements of percent surface irradiance (% SI) and the diffuse light attenuation coefficient (*k*) are made from simultaneous measurements of surface (ambient) and underwater irradiance. Measurements of photosynthetically active radiation (PAR = ca. 400 to 700 nm wavelength) are collected on the surface using an LI-190SA quantum-sensor that provides input to a LI-COR datalogger (LI-COR Inc., Lincoln, Nebraska, USA). Underwater measurements are made using a LI-192SA or LI-193SA sensor. Measurements of % SI and *k* are based on three or more replicate determinations of instantaneous PAR collected by surface and underwater sensors and recorded by the datalogger. Care is taken to reduce extraneous sources of reflected light (from boats or clothing).

Light attenuation will be calculated using the transformed Beer Lambert equation:

$Kd = -[\ln(Iz/I0)]/z$

where *k* is the attenuation coefficient (m-1) and Iz and I0 are irradiance (µmol photons m-2 sec-1) at depth z (m) and at the surface, respectively.

Percent surface irradiance available at the seagrass canopy will be calculated as follows:

$\% SI = (Iz/I0) \times 100$

where Iz and I0 are irradiance (µmol photons m-2 sec-1) at depth z (m) and at the surface, respectively.

A.3 Seagrass Tissue Nutrient and Isotopic Analysis

Developed by: Kenneth Dunton, Kimberly Jackson, Christopher Wilson, Karen Bishop and Sang Rul Park
Last updated: December 2009
Approved by: EPA (2002) and TPWD (2010)

Tissue C:N Content, $\delta^{13}C$ and $\delta^{15}N$

Newly formed leaves (the youngest leaf in a shoot bundle) are gently scraped and rinsed in tap water to remove algal and faunal epiphytes. The rinsed tissue samples are then dried to a constant weight at 60 °C and homogenized by grinding to a fine powder using a mortar and pestle. Tissue samples are analyzed for carbon and nitrogen concentrations and isotopic values using either a Carlo Erba 2500 elemental analyzer coupled to a Finnigan MAT DELTAplus Isotope Ratio Mass Spectrometer 23 (UTMSI; precision 0.3 ‰).